8-2022

Impacts of Summer Drought and Climate Change Conditions on Hydropower Resources and Power System Reliability in the PJM Region

William J. Tingen II
University of Tennessee, Knoxville, wtingen@vols.utk.edu

To the Graduate Council:

I am submitting herewith a thesis written by William J. Tingen II entitled "Impacts of Summer Drought and Climate Change Conditions on Hydropower Resources and Power System Reliability in the PJM Region." I have examined the final electronic copy of this thesis for form and content and recommend that it be accepted in partial fulfillment of the requirements for the degree of Master of Science, with a major in Electrical Engineering.

Kevin L. Tomsovic, Seddik M. Djouadi, Major Professor

We have read this thesis and recommend its acceptance:

Kevin L. Tomsovic, Seddik M. Djouadi, Fangxing Li

Accepted for the Council:
Dixie L. Thompson

Vice Provost and Dean of the Graduate School

(Original signatures are on file with official student records.)

Impacts of Summer Drought and Climate Change Conditions on Hydropower Resources and Power System Reliability in the PJM Region

A Thesis Presented for the

Master of Science

Degree

The University of Tennessee, Knoxville

William Jerome Tingen II

August 2022

Acknowledgments

I would like to express my sincerest gratitude to my advisors, Dr. Kevin Tomsovic and Dr. Seddik Djouadi, for taking me on as a student and offering their guidance and support throughout this process.

I would like to thank Dr. Fran Li and Dr. Hang Shuai for their support on this project and helping me get up to speed with their work in this area, and for their generous and thoughtful feedback.

I would also like to thank CURENT, the Center for Ultra-Wide-Area Resilient Electric Energy Transmission Networks, for providing me with research, outreach, and industry opportunities that continued sparking my interest in the power sector.

Lastly, I would like to thank my wife Emily, family, and friends (especially Rebecca Brink) for their continued support and encouragement during my time as a master's student.

Abstract

The United States power grid is a large, complex, and interconnected system that involves the coordination of numerous entities (e.g., power plant owners/operators, regulators, stakeholders, etc.). As such, any type of extreme event can potentially threaten the economic, safe, and reliable operation of the grid. One such example is summer drought (i.e., events predominantly characterized by elevated temperatures and reduced precipitation), which have impacts spanning all aspects of the power system, especially generation resources through changes in water availability and temperature. Additionally, although heavily dependent on region, climate change can potentially increase the likelihood and severity of drought conditions, illustrating the necessity for understanding the potential impacts of droughts within a climate change context. Accordingly, our analysis investigated the impacts of nine drought and climate change conditions on hydropower plants in the PJM region as of 2030, relative to a historical baseline, using the Hydrologic and Water Quality System (commonly referred to as HAWQS). We found that the historical drought of 2007 was the worst-case scenario in terms of overall generation reduction, followed by proposed 2030 moderate and severe climate change drought conditions, respectively. Because the most similar technology to hydropower is natural gas combustion turbines (in terms of ancillary grid services), replacement of lost generation can induce significant economic consequences for the region's electricity producers and consumers alike. Furthermore, impacts also affect broader grid reliability via reduced generation capacity available to satisfy electricity demand — this was found to not be an issue in the forecasted 2030 PJM generation fleet, but if coal plant retirement is accelerated beyond current plans, then an inability to satisfy peak demand becomes apparent across most scenarios post 50% retirement.

Table of Contents

List of Tables

List of Figures

Nomenclature

$\%\Delta$	percent change
η	plant efficiency
ρ	freshwater density
$AOGCM$	Atmosphere-Ocean General Circulation Model
AVL	Availability
AVL_{hist}	historical availability
AVL_{new}	drought/climate change availability
C_i	available capacity
cmd	cubic meters per day
cmh	cubic meters per hour
$CMIP5$	Coupled Model Intercomparison Project Phase 5
cms	cubic meters per second
$DEWS$	Drought Early Warning System
E	evapotranspiration amount
$eDNS$	Expected Demand Not Supplied
$eENS$	Expected Energy Not Supplied

EHA	Existing Hydropower Assets
EIA	Energy Information Administration
$ELCC$	Effective Load Carrying Capacity
ESM	Earth Systems Model
$ESRI$	Environmental Systems Research Institute
FOR	Forced Outage Rate
ft	foot
g	gravitational acceleration constant
GIS	Geographic Information System
GW	gigawatt, or 10^6 watt
H	hydraulic head
$HAWQS$	Hydrologic and Water Quality System
HT	High-Top Atmosphere
HUC	Hydrologic Unit Code
HYC	Conventional Hydropower
kg	kilogram, or 10^3 gram
L_i	expected load
$LCOE$	Levelized Cost of Energy
$LOLP$	Loss of Load Probability
m	meter
mm	millimeter, or 10^{-3} meter

MW	megawatt, or 10^3 watt
MWh	megawatt-hour
n	number of generators
NID	National Inventory of Dams
$NIDIS$	National Integrated Drought Information System
$NOAA$	National Oceanic and Atmospheric Administration
$NWIS$	National Water Information System
$ORNL$	Oak Ridge National Laboratory
P	percolation amount
P_i	probability
P_{cap}	installed capacity
$P_{day,total}$	total daily generation
P_{hist}	historical total daily generation
P_{new}	drought/climate change total daily generation
PJM	Pennsylvania, New Jersey, and Maryland Power Pool
PSH	Pumped Storage Hydropower
$Q_{day,avg}$	daily average flow
Q_{design}	design flow
Q_{ret}	return flow amount
Q_{surf}	surface runoff amount
R	precipitation amount

RCP	Representative Concentration Pathway
RoR	Run-of-River Hydropower
s	second
SW	soil water content
$SWAT$	Soil and Water Assessment Tool
t	time
$U.S.$	United States
$USACE$	United States Army Corps of Engineers
$USGS$	United States Geological Survey
VIC	Variable Infiltration Capacity
W	watt

Chapter 1

Introduction

The economic, safe, and reliable operation of our power system encompasses the coordination of numerous entities and resources, often involving interdependent and interrelated components [10, 11, 12, 13, 14]. Extreme weather events have historically been the most common cause of power system disruptions, and climate change only threatens to increase their likelihood and severity, which have both economic and public health and safety impacts [15, 16, 17, 18, 19]. For instance, droughts (i.e., events typically characterized by reduced precipitation and elevated temperatures) can reduce water availability for power generation while simultaneously increasing the electricity demand of consumers [10, 11]. Accordingly, when conducting analyses on the impacts of extreme weather events on the power system, addressing the key components of the underlying system dynamics is important to adequately characterize the system itself, and ensure realistic and applicable results [12].

This chapter gives a brief overview of subject matter of this thesis (Section 1.1), the motivation for pursing the presented analysis (Section 1.2), and the overall structure of the subsequent chapters (Section 1.3).

1.1 Overview

Throughout the past few decades, the United States (U.S.) power system has experienced numerous extreme weather events (e.g., droughts, polar vortexes, hurricanes, etc.) that demonstrated clear vulnerabilities across each of its components (i.e., the generation,

transmission, and distribution sectors) [18]. The main direct and indirect pathways of these impacts are illustrated in Figure 1.1, along with some of the relevant competing users of the particular resource [11, 20, 21, 22, 23, 24]. One of the central themes in these vulnerabilities is that these systems were designed to withstand current and historical conditions, and have limited adaptive capabilities to handle more volatile and severe weather conditions, which are only expected to worsen under most climate change scenarios [16, 17, 18, 25]. Specifically, each of the different generation resources (e.g., thermal, hydro, solar, wind, etc.) has their own set of constraints that limit their operational flexibility under normal circumstances, that are only further exacerbated and compounded in extreme weather events [17, 18, 26]. For instance, both hydro and thermal power plants require a water supply to generate electricity [1, 16, 17, 25, 26, 27]. Therefore, reduced water availability (i.e., streamflow) and increased water temperature resulting from drought conditions, where the former impacts both types and the latter mainly impacts thermal (i.e., only select hydro plants with water temperature environmental constraints are also affected), can cause plants to completely, or at least partially, curtail operations [1, 16, 17, 25, 26, 27]. Specific extreme weather events include the 2007-08 Southeastern drought, 2011 Texas drought, and 2014 Northeastern polar vortex, among many others of varying severity [1, 5, 11].

One such event that has been garnering much attention recently has been droughts — researchers across the U.S. and world have been looking into the range of potential impacts on their respective power systems [10, 11, 16, 17, 23, 28, 29, 30, 31]. In the U.S., Texas and the Western Interconnect have been the predominant subject of most research, due to the historical arid, drought-prone climate conditions, leaving the Eastern interconnect to receive much less attention [10, 11, 23, 28, 29, 31]. Accordingly, due to the readily available, public data [1] and system literature available related to system operations, reliability, and resilience, this paper focuses on the Pennsylvania, New Jersey, and Maryland Power Pool, or PJM Interconnection (which will be referred to as PJM henceforth) [5, 32, 33, 34]. Of the many resources comprising the power system, hydropower has been identified as extremely vulnerable to severe reductions in generation capacity from drought conditions, which can have severe implications on system revenue due to hydropower typically having lower

[1] PJM Data Miner 2: https://dataminer2.pjm.com/list

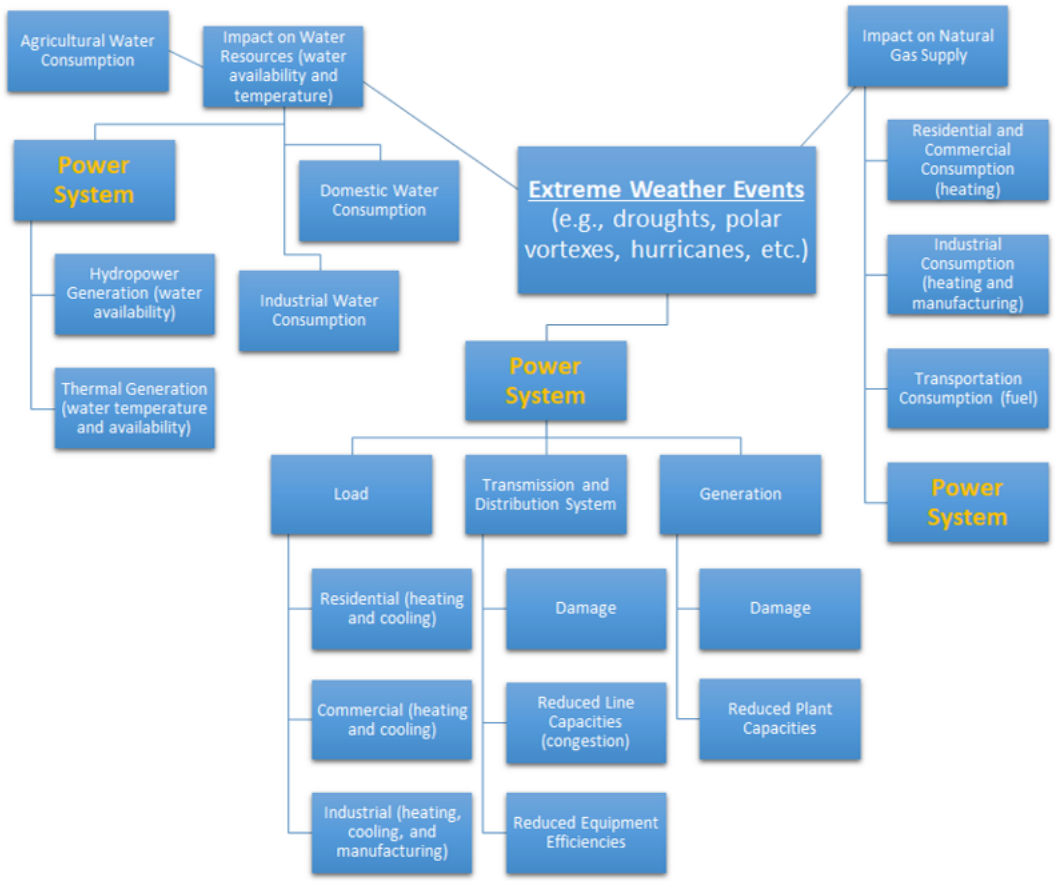

Figure 1.1: Extreme weather events can impact the power system directly and indirectly via fuel supplies and water resources, which are subject to competition between various users.

operating costs than other resources, as well as grid reliability due to hydropower providing many ancillary services [5, 30, 11, 23, 10, 16, 17, 13, 28, 35, 36, 27].

1.2 Motivation

As discussed briefly in Section 1.1, hydropower resources are directly dependent on water availability to generate electricity and thereby, any disruptions to this supply can have larger system impacts far beyond just curtailed operations of the plant. For instance, reductions in hydropower generation necessitate that other generation resources will need to increase their output to compensate for the loss in order to continue satisfying electricity demand, which could then increase energy prices due to the typically lower operating costs of hydropower compared to other resources (e.g., coal, natural gas, etc.) [23, 37, 38]. Additionally, hydropower provides many ancillary grid services that are vital to system stability and security (e.g., voltage and frequency regulation, black start capability, etc.), which would then need to be replaced by another resource, or even multiple other resources, most likely at a higher price [5, 35].

1.3 Organization

This thesis discusses the vulnerability of the U.S. power grid to summer drought conditions and climate change, specifically detailing the impacts on hydropower resources, revenue streams, and broader grid reliability in the PJM region.

Chapter 2 presents background information relevant for understanding droughts and climate change, and how they can impact the power system, particularly in terms of hydropower resources and broader grid reliability.

Chapter 3 discusses the methodology for modeling hydrologic conditions throughout PJM, under historical and our proposed drought and climate change conditions.

Chapter 4 describes how the results of the hydrologic modeling were translated into quantifiable impacts on the PJM hydropower fleet, along with the corresponding impacts on system revenue and broader grid reliability.

Chapter 5 summarizes of the results of this analysis and highlights key conclusions.

Chapter 6 identifies areas of future work, where our methods and assumptions can be further refined and expanded upon.

Chapter 2

Background

In order to quantify the impacts of drought and climate change on hydropower resources in the PJM region, understanding what exactly constitutes a drought, how climate change threatens to worsen drought conditions in the future, and how these conditions will conceptually impact hydropower resources and the broader power system is paramount. Accordingly, this chapter covers several background topics related to understanding the context of our analysis, including:

- The interdependencies between water and the power system, the definition of a drought, the relationship between climate change and drought, and accordingly, how drought affects the overall power system (Section 2.1);
- The different types of hydropower and their role in the power grid (Section 2.2); and
- The history of PJM, in terms of its organizational structure and drought vulnerability, and its current hydropower fleet (Section 2.3).

2.1 Drought, Climate Change, and the Power System

Water is a central underlying element of our modern economy and thereby, scarcity prompted by drought and worsened by climate change has the potential to have severe impacts across numerous sectors due to competing water demands, especially if demand is expected to increase in the coming years from population growth [1, 10, 17, 24, 27, 39, 40]. Per the

U.S. Geological Survey (USGS), water usage can be divided into several main categories, each with differing levels of consumption (as of 2015): domestic (13% spread across public and private usage), agriculture (40% spread across irrigation, livestock, and aquaculture usage), industrial (5%), mining (1%), and thermal power production (41%) [41]. The latter of which constitutes the largest percentage of water consumption, followed closely by agriculture, which then implies a major interdependence between power and water supply, and considerable potential for competition in times of water shortages. Thermal power is primarily characterized by boiling water to create steam via either the burning of a fuel source (e.g., coal, oil, biomass, etc.), utilizing the heat byproduct of a process (e.g., nuclear, combined-cycle natural gas, etc.), or through some other means typically involving a specific type of renewable energy (e.g., concentrating solar, geothermal, etc.) [42, 43]. This steam is then used to spin turbine-generators, which are turbines with generators attached to their shafts, to produce electricity (i.e., through mechanical-to-electrical energy conversion, where the mechanical energy consists of more kinetic than potential), and before the steam can be reused, it must be recondensed back into water [42, 43, 44]. Accordingly, this sector's consumption is primarily related to the boiling and recondensing processes [42, 43].

Even though hydropower isn't included in water consumption as no water is actually consumed (i.e., water is simply passed through the turbine-generators of a facility to generate electricity), water scarcity, or drought, still threatens to heavily impact hydropower solely via reductions in water availability [1, 5, 10, 11, 13, 16, 17, 23, 24, 27, 28, 30, 35, 36]. Specifically across 2006 to 2013, there were numerous cases of thermal and hydro plant curtailments across the continental U.S. solely due to water issues, as illustrated by Figure 2.1 [1]. In extreme instances, curtailments can result in localized brownouts and blackouts, exemplified by major coal plant shutdowns during the Summer of 2007 in North Carolina [1]. Therefore, the impacts of water-related problems on the power system can be grouped into three main categories, which then result in derated capacities, lower efficiencies, and/or shorter generation availability periods, detailed below and summarized in Figure 2.2 [1, 10, 24, 25, 42, 43]:

1. Changing the supply available for hydropower and thermal power generation;

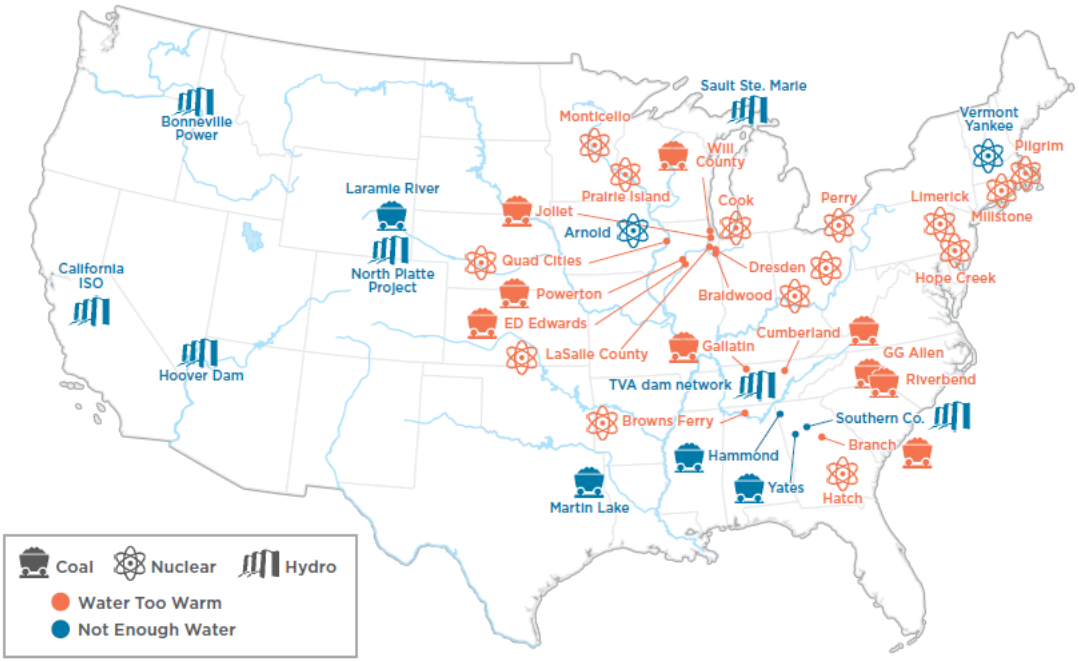

Figure 2.1: U.S. thermal and hydro power plants that experienced curtailment due to water-related issues from 2006 to 2013 [1].

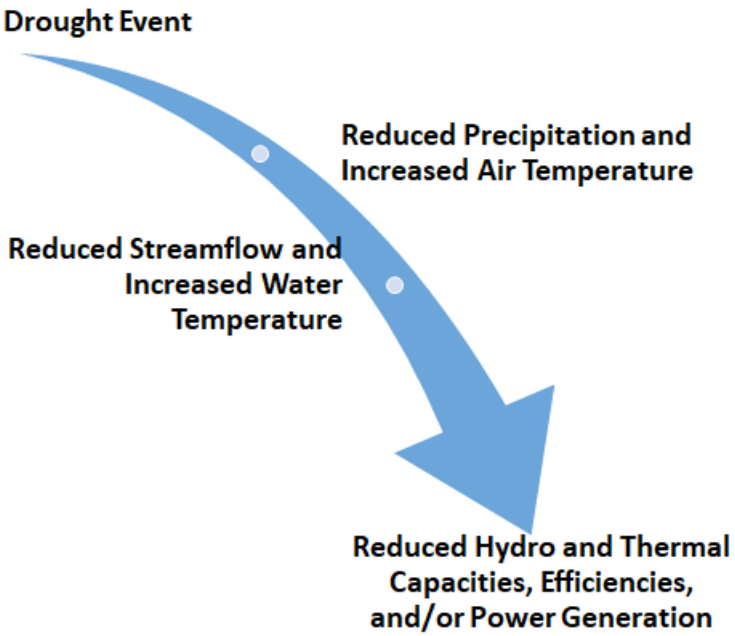

Figure 2.2: Typical pathway of droughts impacting the power system with respect to hydro and thermal power plants.

2. Changing the supply available for thermal plant cooling processes; and

3. Changing the intake water temperature for thermal plant cooling processes — certain types of thermal plants discharge used cooling water back into the nearby river, typically at elevated temperatures (i.e., hotter water in, hotter water out), and there are regulatory standards on the upper limits of these temperatures.

In order to understand and quantify the impact of droughts and climate change on the power system, a clear definition of what exactly constitutes a drought and the relationship between climate change and droughts are necessary. Accordingly, there are several main categories of drought, dependent on the specific variable(s) being measured: meteorological (precipitation), agricultural (soil moisture), hydrologic (streamflow and groundwater), and socioeconomic (economic water demand) [11]. Because streamflow is directly related to electricity generation for both hydro and thermal plants, a hydrologic drought was chosen for this study, which follows that of previous studies [10, 11, 16, 17, 23, 30, 36]. Furthermore, streamflow can be considered the "end-product" of a watershed — it incorporates a range of conditions from meteorological (e.g., precipitation) to agricultural and domestic consumption, as well as general basin processes (e.g., water transfer and storage) — and thereby, measuring streamflow can illustrate the overall system's condition [11]. Additionally, droughts are often characterized according to duration, frequency, severity, spatial extent, and temperature deviation [11]. All of these parameters can vary widely so there is no consistent measure for a typical drought scenario, especially when coupled with regional variability in weather and climate conditions [11, 23, 30].

Similarly, there is no typical climate change scenario — many variations exist in the types of models available for analysis and the inherent assumptions contained within (specifically with respect to greenhouse gas emissions and environmental processes included in the model formulation), and by definition, these are projections of the future so they are inherently subject to uncertainty [9, 45]. However, climate change is still expected to heavily impact water resources and broader hydrology across the globe, typically through increases in air temperature and changes in precipitation patterns that can affect evapotranspiration, water temperature, streamflow quantity, and runoff patterns (particularly in size and timing),

among many others [1, 19, 25, 39, 40, 46, 47]. Specifically, changes in precipitation and runoff patterns can lead to shorter periods of more intense rainfall (which then induces flooding, meaning additional flood mitigation measures must be adopted), separated by longer periods of no rainfall, or drought conditions [19, 24, 40, 46]. Unfortunately, climate change is exemplified by regional variability, complicating the analysis and evaluation of potential impacts, largely due to available data resources and regionally relevant models [1, 19, 27, 36, 40, 47].

Therefore, droughts and climate change can have direct impacts on the power system across all three water-related avenues discussed previously — i.e., reductions in water supply available for both power generation and thermal plant cooling processes, and increases in water temperature for thermal plant cooling processes [1, 10, 16, 17, 24, 25, 42, 43]. Furthermore, reductions in generation efficiencies from water shortages imply that additional electricity must be produced to compensate for the loss, noting that operation at non-optimal efficiencies can increase equipment degradation, both leading to increased overall system operational costs and risks of failure [11, 48]. However, the effects of drought and climate change can extend beyond the generation component of the power system. For instance, electricity demand (also referred to as load) tends to be highest in summer when temperatures are greatest, which would only be further exacerbated by drought and climate change (i.e., via associated increased temperatures) [1]. Additionally, higher temperatures decrease the thermal loading limits of transmission and distribution systems (i.e., both power lines and circuit breakers), while also increasing system losses and overall operational costs [11, 48]. With these concerns in mind, drought and climate change can have serious implications on the economic, safe, and reliable operation of our power system and therefore, the potential range and extent of these impacts must be analyzed and addressed.

2.2 Hydropower

Generally speaking, hydropower (also called hydroelectric power) uses moving water to generate electricity, and is one of the oldest forms of energy production across the world [37]. The specific means of generating energy can vary across different plants, as well as the

specific method of dispatchment in the power system; however, most plants can be grouped into three main categories: impoundment or conventional (HYC), run-of-river (RoR) or diversion, and pumped-storage (PSH) [2]. While each type has their own advantages and disadvantages in regards to construction and operation, they are all extremely useful in the reliable and economic operation of the power system, as they provide many reliability and resiliency benefits while still being a renewable and clean energy resource [49].

2.2.1 Types of Hydropower Plants

HYC plants are the most common type of hydropower facility and involve the complete impoundment of a flowing water source (i.e., damming of a river or stream) to amass potential energy (usually referred to as hydraulic head) for power generation [2, 37, 50]. Accordingly, the inclusion of significant sources of both kinetic and potential energy at these facilities greatly increase the amount of power that can be generated (also known as a plant's installed capacity) [37, 44, 50]. This impoundment, which varies from dam-to-dam in terms of materials and design due to site-specific conditions, creates a reservoir, where water can be stored for various purposes (e.g., power generation, flood control, domestic water supply, recreation, etc.) [50]. For power generation purposes, water from the reservoir is conveyed through one or multiple penstocks to a powerhouse, spinning turbine-generators to generate electricity, where it is then released downstream into the facility's tailrace [2, 50]. HYC plants also have other structures that allow for additional releases of water, typically unrelated to power generation such as passing flood water or debris, maintaining environmental flows, and facilitating fish migration, among many others [50]. Refer to Figure 2.3 for a sample schematic of a HYC facility.

On the other hand, RoR plants tend to avoid the complete impoundment of a river by instead diverting a portion of the water through a canal, which then feeds a penstock conveyance system to a powerhouse, as illustrated by Figure 2.4 [2, 49, 51]. Occasionally a partial impoundment of the river is included to facilitate water entering the penstock, but typically this provides little more than same-day storage (i.e., no future use) [49, 51]. To be viable, the river must have a substantial and consistent year-round flow rate, which can be bolstered by any natural elevation difference (i.e., potential energy), as RoR facilities

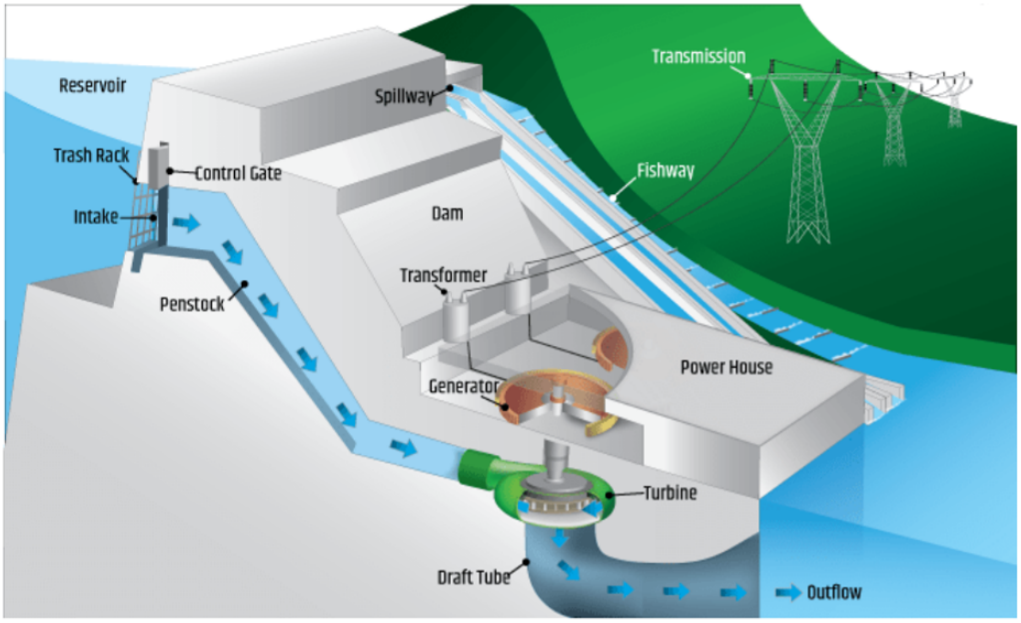

Figure 2.3: Sample schematic of a conventional hydropower facility (not to scale) [2].

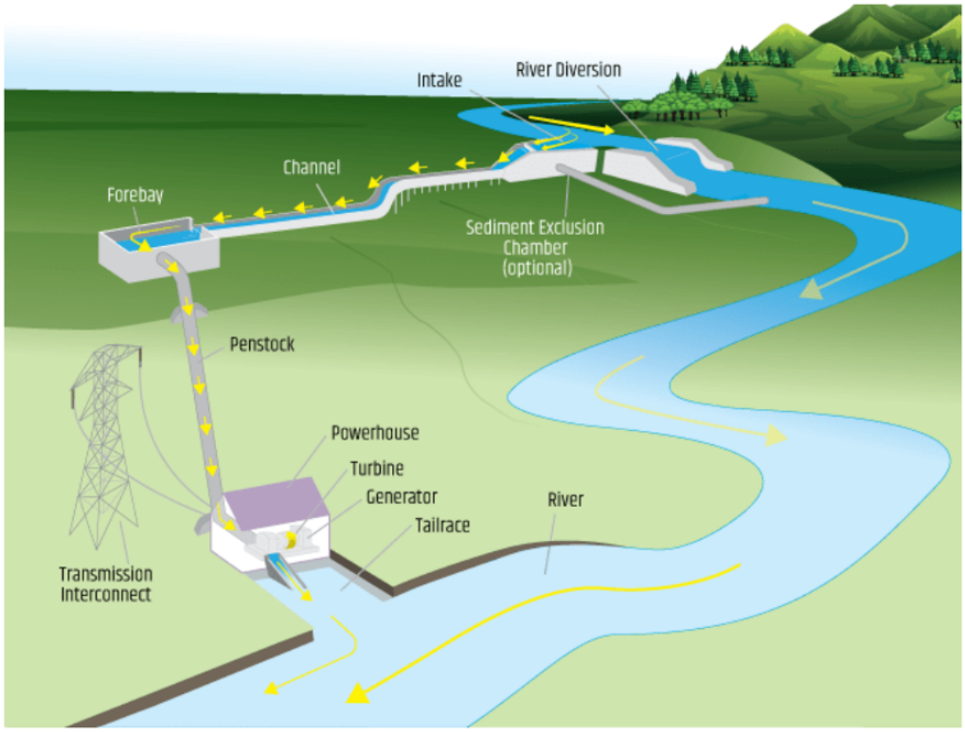

Figure 2.4: Sample schematic of a run-of-river hydropower facility (not to scale) [2].

are designed to operate at the most common flow rate, essentially wasting any larger flows [2, 49, 51]. Compared to HYC facilities, RoR tend to be less expensive, much easier and quicker to build, pose fewer environmental problems, and allow for more flexibility with siting, as most of the optimal sites for HYC plants have already been utilized [51]. However, typically the installed capacity of these plants is significantly lower than that of HYC facilities, and they are typically less reliable for power generation due to their inherent operational strategy, meaning that even though the initial capital costs may appear lower than HYC plants, the cost per MW can be higher [51].

Quite unlike HYC and RoR, PSH essentially works as a giant "water battery" — a penstock system and powerhouse, which contains turbine-generators and pump systems, connect two impounded reservoirs sited at different elevations [2, 3, 49]. Refer to Figure 2.5 for a sample schematic of a PSH facility. Typically during periods of low electricity demand, where the price of energy is also low (usually late night and early morning hours), water is pumped from the lower reservoir into the upper, and then when demand and prices peak, that water is released back down into the lower reservoir to generate electricity [2, 3, 49]. Accordingly, PSH plants tend to have greater operating costs compared to RoR and HYC since more electricity is consumed during pumping than is made during generation (i.e., the roundtrip efficiency is approximately 75%); however, economies of scale and peak energy prices tend to offset these costs, which is commonly referred to as energy arbitrage [3]. There are two main configurations of PSH facilities, open-loop and closed-loop, that are mainly distinguished by their continual connectedness to a naturally flowing water source (i.e., open-loop is connected and close-loop is not) [3]. Across the U.S., PSH plants supply approximately 95% of utility-scale energy storage using only 43 plants (most of which are open-loop and extremely large with respect to installed capacity), and greatly simplify the integration of intermittent renewables like solar and wind into the power grid, in addition to providing many grid reliability and resiliency benefits [3].

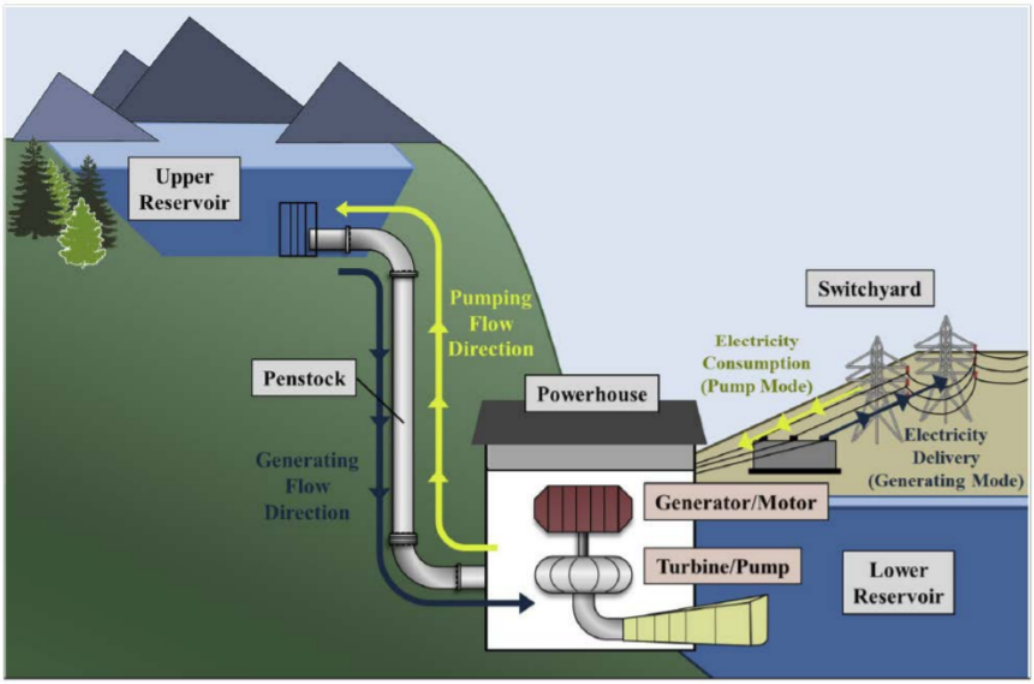

Figure 2.5: Sample schematic of a pumped storage hydropower facility (not to scale) [3].

2.2.2 Hydropower Grid Benefits

In the U.S. and across the globe, hydropower is the predominant renewable energy technology, providing the bulk share of renewable generation throughout the past century, and has only just recently been overtaken by wind power in the U.S. (in terms of annual generation) [35, 52]. Additionally, unlike some other renewable resources (e.g., intermittent solar and wind), hydropower can provide many ancillary grid services that support grid stability, reliability, and resiliency, including [3, 5, 35, 53, 54, 55]:

- Synchronous Reserve (online generators that can quickly respond to changes in load).
- Non-Synchronous Reserve (offline generators that can quickly come online to provide power).
- Frequency Regulation (ability of a generator to assist in correcting frequency mismatches, which occur due to power imbalances between electricity supply and demand) through:
  - Inertia, or the kinetic energy stored in large rotating masses (i.e., turbines), essentially acts as a shock-absorber that reduces the immediate impact of rapid changes in load, buying time for automatic control systems to detect and respond to the system change.
  - Primary Frequency Regulation, which entails the automatic adjustment of power output via turbine governor control systems.
  - Secondary Frequency Regulation, which involves manual adjustment of power output by system operators.
- Load-Following Capability (ability of generator to quickly adjust power output to match load, which encompasses quick start-up times and low minimum run times).
- Reactive Power and Voltage Support (ability of generator to absorb and/or generate reactive power to maintain voltage stability, or voltages at desired levels).
- Black-Start Capability (ability of a generator to start-up independent of the larger power system, which is extremely useful following blackout events — typically, a hydro

plant only needs a small power source to open the gate(s) preventing water from entering the penstock and reaching the turbine-generators).

While not every hydropower plant can offer all of these services, as they are largely dependent on the specific size and type of plant in question, as well as the level of operational constraints that have been imposed by competing water uses (e.g., domestic, industrial, and agricultural consumption, recreation, environmental, etc.), together as a unit, hydropower is a major player in facilitating the safe, economic, and reliable operation of our power grid [3, 35, 54]. For instance, while hydropower represents less than 6.7% of U.S. generation capacity, it tends to provide a disproportionate amount of black start capability (nearly 40%), frequency regulation, generation reserves, and load-following capability compared to other resources, even in regions with fewer hydropower resources such as PJM [55].

2.3 PJM Interconnection

Originally formed in 1927, when three neighboring utilities joined their generation resources together to reduce operating costs and improve system efficiencies, PJM has since evolved to become an independent, third-party organization that oversees and coordinates the movement and sale of electricity throughout a large part of the Northeastern U.S. [56, 57]. Its territory encompasses several entire states and parts of many more, totaling 369,089 square miles across 13 states and the District of Columbia, as illustrated in Figure 2.6 along with PJM's major operating zones (i.e., subdivisions surrounding specific load centers) [56, 58, 59]. Contained in this region are approximately 65 million people served through more than 85,000 miles of transmission lines that are responsible for nearly 21% of the U.S. gross domestic product [59]. Membership in PJM covers both utilities and non-utilities, spanning five main categories: generation resource owners, transmission system owners, distribution system owners, consumers, and miscellaneous suppliers (i.e., organizations that provide energy supporting services) [56]. Many companies are included in PJM, from the Commonwealth Edison Company to Pennsylvania Electric to Dominion Energy, totaling more than 1,040 members [57, 59]. While these companies do have their own operational area, they constantly interact with one another to produce and provide electricity to the

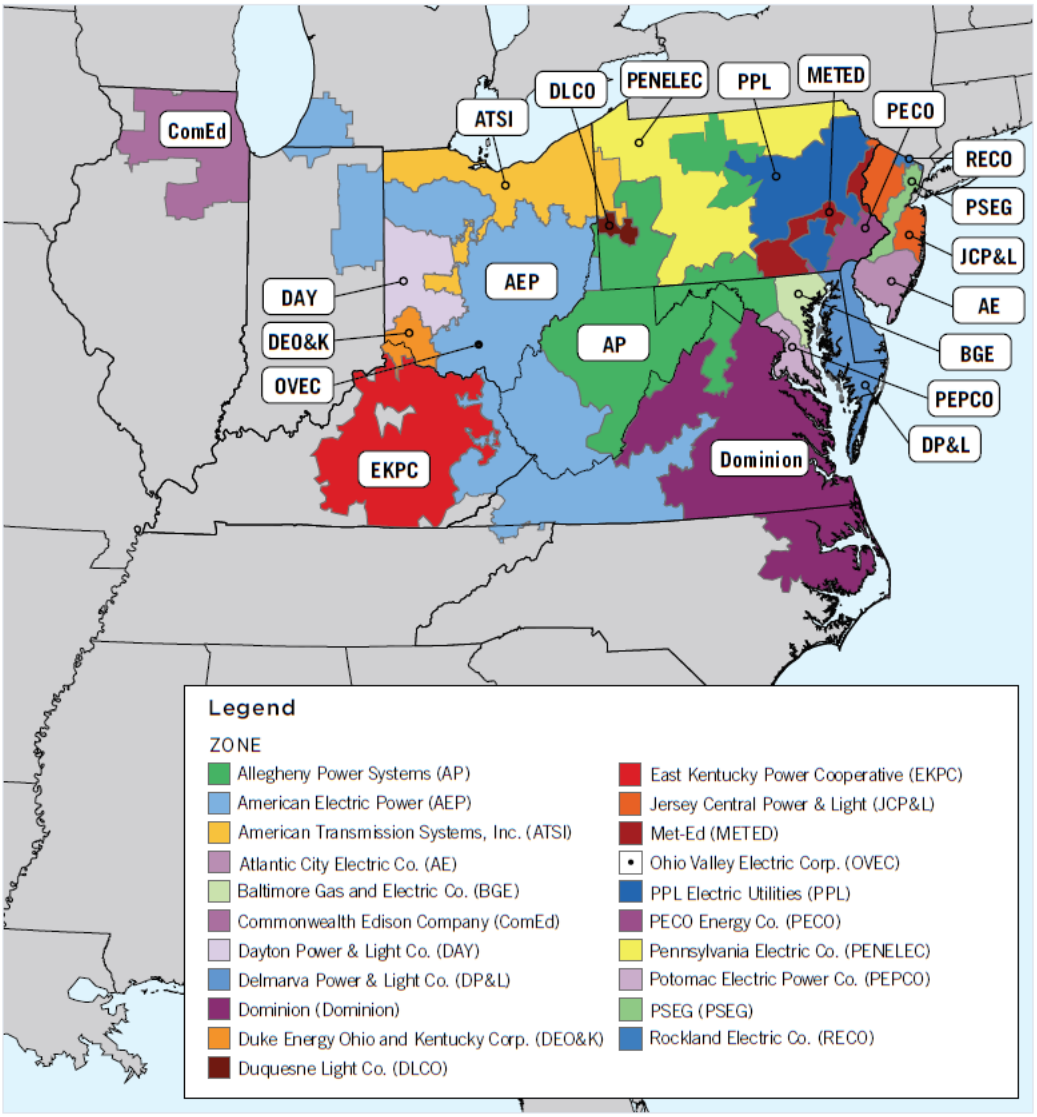

Figure 2.6: Map of PJM's territory and major operating zones [4].

consumers of this region [56, 57]. Accordingly, PJM is an extremely important region of the U.S., further validating the necessity for understanding the potential impacts of droughts and climate change on its power system.

Since its inception, PJM's generation fleet has undergone numerous changes following different nationwide and regional trends in development, becoming increasingly diversified throughout time [5]. For instance, just in 2005, coal and nuclear resources constituted nearly 91% of generation, but have dropped to approximately 55% by 2020, largely due to coal plant retirements and increased development in natural gas resources [5, 60]. Likewise, over the past two decades, the dominance of coal power in terms of installed capacity has been steadily declining and overtaken by natural gas, as shown in Figure 2.7 [5]. Extending across the past 80 years, additional trends and insights driving generation diversity can be deduced, such as the impacts of various policies (e.g., air quality and environmental regulations, renewable energy portfolio standards, etc.) and extreme events (e.g., Three Mile Island Nuclear Accident, 1970s oil crisis, etc.) [5]. Additionally, hydropower is shown to be apart of the original generation mix, with its contribution to total generation decreasing over time as PJM's population and territory grew, and as other resources can online [5]. However, it is important to note that hydropower still plays a clear role in modern days, both in providing generation and ancillary services to maintain grid stability and reliability, as well as providing renewable energy to reduce greenhouse gas emissions, which is increasingly important to combat climate change (also many states within PJM have set renewable energy portfolio standards that hydropower can help satisfy) [5, 55]. These trends and more are shown in Figure 2.8.

2.3.1 PJM Hydropower Fleet

Information regarding PJM's hydropower fleet, which is defined as all plants listing PJM as their balancing authority per the Energy Information Administration (EIA), was primarily obtained from two databases, the Oak Ridge National Laboratory (ORNL) HydroSource Existing Hydropower Assets (EHA) Plant Capacity Database[1] and EIA Form 860

[1]ORNL HydroSource EHA Plant Capacity Database: https://hydrosource.ornl.gov/dataset/existing-hydropower-assets-eha-capacity-plant-database-2005-2019/

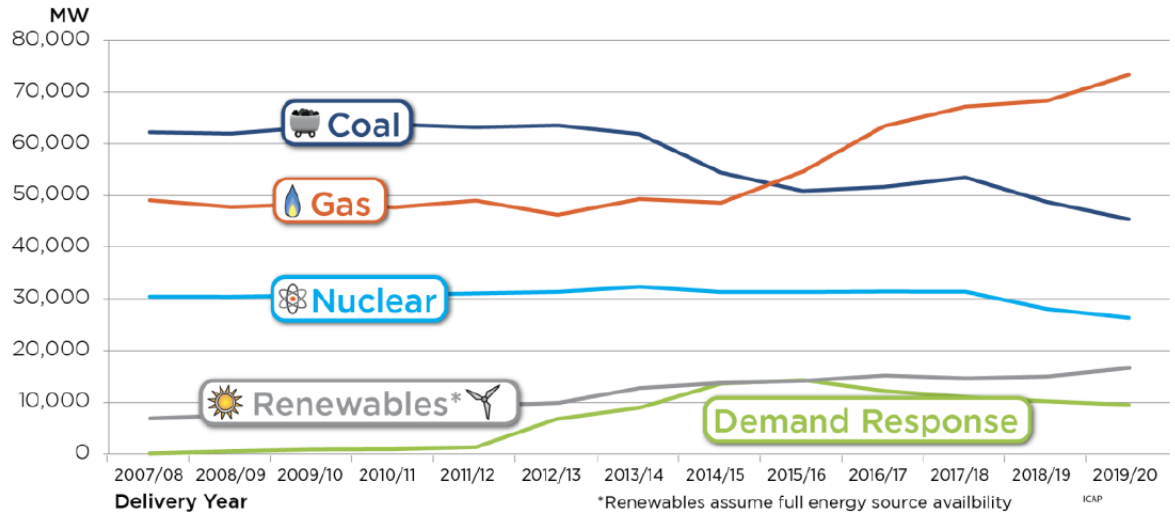

Figure 2.7: Distribution of installed capacity by generation resource type in PJM across 2007-2019 [5].

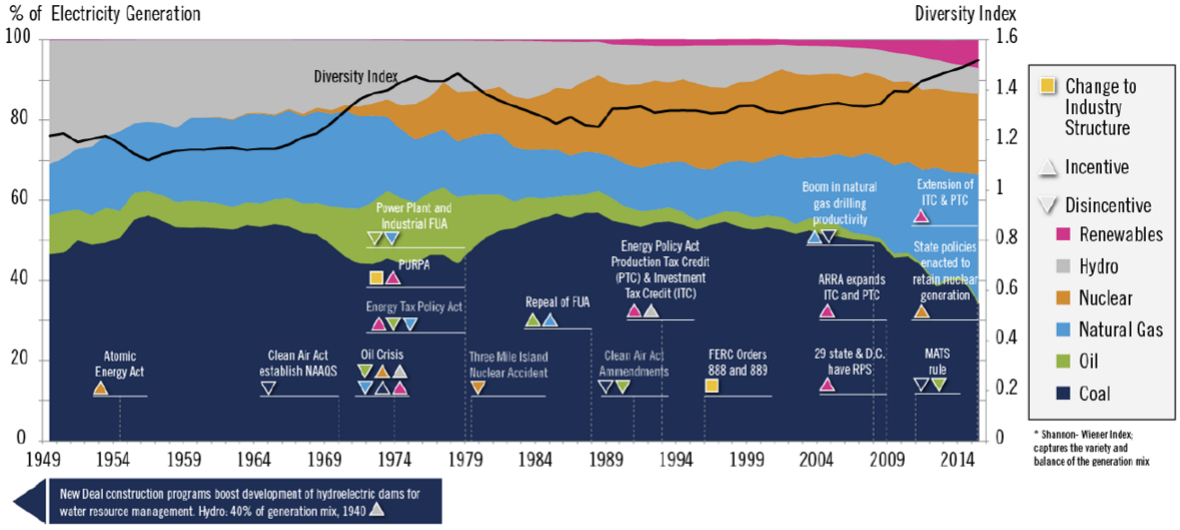

NOTE: This graphic is not an exhaustive representation of all drivers related generation mix change. The intent was to capture examples of major drivers, with a focus on policies and events that targeted specific resource types.			
NAAQS	National Ambient Air Quality Standards	ARRA	American Recovery & Investment Act
PURPA	Public Utility Regulatory Policies Act of 1978	RPS	Renewable Portfolio Standard
FUA	Power Plant and Industrial Fuel Use Act of 1978	MATS	Mercury and Air Toxics Standards

Figure 2.8: Composition of generation by resource type in PJM across 1949-2014, with indications of significant policy drivers and events that impacted system diversity [5].

Database[2] [61, 62]. Specifically, the ORNL dataset was used to verify and supplement the EIA data, which contained all operational plants, planned retirements, and proposed additional generation (whether in the form of retrofits or new facilities) over the next decade, as envisioned in 2020 [61, 62]. Because this analysis includes the impacts of climate change, PJM's hydropower fleet incorporates these planned retirements and proposed additions, resulting in a projected fleet as of 2030 [61, 62].

Accordingly, PJM's hydropower was found to be widely dispersed across its entire territory, varying greatly with respect to installed capacity, ranging from extremely small (below 1MW) to extremely large (above 1GW). In total, there are 108 hydropower plants above 0.4MW, with five being PSH and the rest being HYC and RoR, with PSH comprising approximately 63% of total capacity and HYC and RoR comprising 37%. Figure 2.9 illustrates this distribution — note that HYC and RoR are combined into one type due to difficulties arising from categorizing each hydropower plant (i.e., lack of available information). For instance, the ORNL dataset defines each plant's operating mode, but many are listed as "unknown," and while denotations of "run-of-river", "peaking", and "reregulating" are useful in understanding more about the plant's operation, they do not exactly correlate with the definitions described in Section 2.2.1 with respect to facility size (e.g., a HYC plant can be operated in RoR mode, but a RoR-style plant is unlikely to exhibit a large dam size and installed capacity). Therefore, to avoid unnecessary error, these denotations were ignored. Additionally, most of the owners and operators of PJM's hydropower plants are local municipalities and private companies, with only a handful being federal projects (e.g., U.S. Army Corps of Engineers [USACE]), and thereby, come under the purview of the Federal Energy Regulatory Commission (FERC) and their licensing and operational rules [63]. For instance, FERC ensures specific environmental and dam safety regulations, in addition to other applicable laws, are followed by all relevant owners and operators, essentially promoting only the construction and operation of facilities that best serve the public, and broader environment, as a whole [63]. Refer to Appendix A for additional information regarding PJM's hydropower fleet.

[2]EIA Form 860 Database: https://www.eia.gov/electricity/data/eia860/

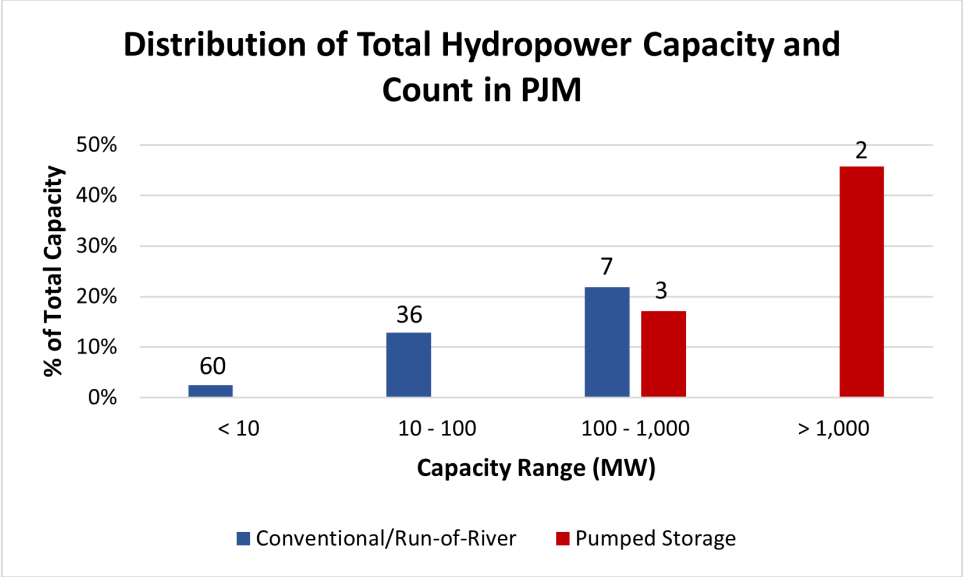

Figure 2.9: Distribution of PJM's 2030 Hydropower Fleet in terms of total capacity and count between pumped storage and joint conventional and run-of-river types.

2.3.2 Drought, Climate Change, and PJM

The National Oceanic and Atmospheric Administration (NOAA) maintains a drought monitoring system for the entire U.S., called the National Integrated Drought Information System (NIDIS)[3], which contains various weather data at varying levels of detail dating back over 2000 years [64]. Using this system, significant drought events affecting PJM can be ascertained; however, because PJM spans such a wide area, it is possible for some regions to experience drought conditions while others undergo normal conditions or even the complete opposite. For instance, in 2007, Kentucky and Virginia experienced extreme and exceptional drought conditions (i.e., D3 and D4 levels according to the NIDIS scale, where D4 is the worst), while Pennsylvania and New Jersey only underwent abnormally dry to moderate drought conditions (i.e., D0 and D1) [65, 66].

The NIDIS also has a subsystem called the Drought Early Warning System (DEWS), which divides the U.S. into several regions and gives more detailed reports of drought conditions, trends, and potential future concerns — in particular, PJM encompasses parts of the Northeast, Midwest, and Southeast regions, as shown in Figure 2.10 [6]. Accordingly, the Northeast region experienced droughts in 2000, 2016, and 2020, and while not typically characterized by long-term droughts, this region is prone to flash-droughts of two to six months in duration [65]. As for the Midwest, significant droughts were experienced in 1998 and 2012, and trends seem to be shifting towards wetter conditions compared to the beginning of the 1900s, albeit with more dramatic swings between dry and wet periods [67]. Lastly, the Southeast has been receiving more record-breaking droughts across the past couple decades, worsened by the typical high temperatures associated with the region, which has lead to increased monitoring efforts and drought mitigation efforts to safeguard against future droughts [66]. As discussed in Section 2.1, climate change has the potential to worsen droughts in already drought-prone areas while inducing droughts in typically drought-less regions; however, there is also potential for conditions improving in some parts, hence the necessity for modeling efforts to characterize the range of potential impacts [9].

[3]NOAA NIDIS: https://www.drought.gov/

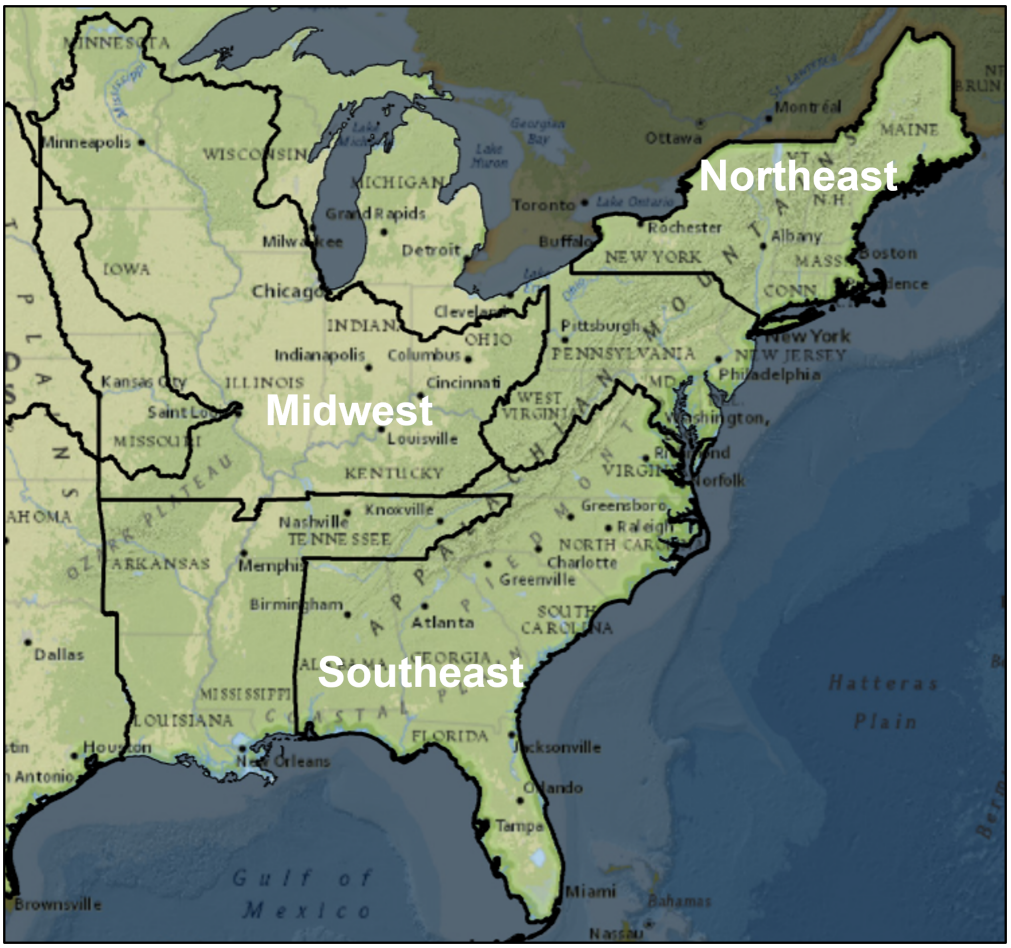

Figure 2.10: Map of the NOAA NIDIS DEWS regions, modified from [6].

.

Chapter 3

Hydrologic Modeling

As discussed in Section 2.1, drought and climate change have a direct pathway for impacting hydropower generation via water availability (i.e., reductions in precipitation and increased air temperature can reduce streamflow and thereby, reduce hydropower generation). Therefore, to best quantify potential impacts of drought and climate change on hydropower, modeling efforts should try to address all aspects of this pathway, especially the underlying environmental processes. Accordingly, this chapter gives an overview of:

- Current hydrologic modeling methods and the specific model chosen for this analysis (Section 3.1);
- The setup and procedure for running this model (Section 3.2); and
- The results of our hydrologic modeling efforts (Section 3.3).

3.1 Hydrologic Modeling Methods

While some approaches to modeling the impact of droughts on power generation resources, whether solely hydro or both hydro and thermal assets, have utilized pre-existing databases such as the USGS National Water Information System (NWIS)[1] or the EIA Form 923[2], the majority of analyses have utilized some type of hydrologic model to estimate the quantity

[1]USGS NWIS Database: https://waterdata.usgs.gov/nwis
[2]EIA Form 923 Database: https://www.eia.gov/electricity/data/eia923/

(i.e., streamflow), and sometimes quality, of water available for electricity production under water-scarce conditions [10, 11, 16, 17, 23, 25, 27, 36, 68]. Typically, the added complexity from employing a hydrologic model in lieu of using historical data stems from either a lack of sufficient, relevant data for the particular site, or the need to test future, or at least non-historical, conditions that are not captured in historical datasets (e.g., climate change scenarios) [10, 11, 16, 17, 23, 25, 27, 36, 68]. The models employed tend to evolve from a similar foundation, where some stochastic or deterministic physically-based process is used to translate weather data into hydrologic responses, such as streamflow, across various temporal scales, usually daily, monthly, or yearly [10, 16, 17, 25, 27, 36, 68]. Two common tools, each having extensive utilization in numerous river basins across the globe and known for accurate and robust estimations, are the Variable Infiltration Capacity (VIC) and the Soil and Water Assessment Tool (SWAT) [69].

VIC is a gridded, process-driven model that converts weather data into hydrologic responses, notably streamflow [27, 69, 70]. These processes encompass surface energy and water balancing, land-atmosphere fluxes, rainfall-runoff modeling, and reservoir operations (however simplistic or complex as necessary), and are performed for each grid-cell independently [27, 69, 70]. The results (e.g., surface and base flows) are then routed together to provide an estimate of streamflow for the gridded network [27, 69, 70]. While not extremely memory-intensive, the VIC model requires many inputs, including extensive weather data; soil, land cover, and vegetation maps; and digital elevation models, all to the appropriate resolution for the analysis at hand, which must be optimized with computational time and efficiency [16, 17, 25, 27, 69, 70].

Similarly, the SWAT model is physically-based, utilizing an extensive array of inputs (e.g., weather, land use, soil, digital elevation models, point and non-point source pollution, etc.) to simulate hydrology, sediment, and contaminant routing throughout a watershed (i.e., both water quantity and quality) [40, 47, 69, 71]. The model encompasses the processes included in the VIC model along with the impacts of sediment and contaminant loading and routing [40, 47, 69, 71]. However, unlike VIC, which is accessed through a programming language (e.g., C), SWAT's user interface is contained within various geographical information systems (GISs), such as the popular Environmental Systems Research Institute (ESRI) ArcGIS

software[3], which facilitates straightforward project construction and simulation [47, 69, 70]. Instead of dividing a watershed into equal-sized gridded cells where all of the processes occur, SWAT delineates a watershed into different subbasins linked together by the river system, which are comprised of multiple hydrologic response units (HRUs), representing different combinations of land covers, soil types, and management practices (a HRU represents the total area constituting a particular combination) [40, 71, 72]. Reductions in computational time are obtained via this delineation process, as all of the unique land, soil, and management combinations are able to be treated jointly as a single unit, rather than multiple separate entities (i.e., it is common for the same HRU combination to be scattered throughout a given region), minimizing the total number of simulations needed as well as the number of unique interactions possible [40, 71, 72].

Due to the extensive modeling framework of SWAT, along with its more user-friendly GIS interface, it was chosen for the basis of this analysis [69, 71]. However, since project initialization and simulation is still quite labor-intensive, specifically in terms of data acquisition, preprocessing, and incorporation, the Hydrologic and Water Quality System (HAWQS)[4] can be employed to streamline the modeling process [71, 73, 74]. HAWQS has a web-based user interface containing all of the necessary input data, options to modify certain aspects of the particular watershed and input data, and data visualization tools to quickly process model outputs [73, 74, 75]. Additionally, identifying watersheds to study is straightforward — maps allow the selection of one or multiple subbasins at three different watershed scales, differentiated by hydrologic unit codes (HUCs) of descending size 08, 10, and 12 (e.g., a HUC-08 region can be subdivided into a HUC-10 region and then further subdivided into a HUC-12 region) — although, only the continental U.S. has been currently incorporated [74, 75].

3.1.1 Additional Detail about HAWQS

Since the foundation of HAWQS is the SWAT model, understanding the core equations and algorithms of SWAT is necessary for utilizing HAWQS. Accordingly, a central distinguishing

[3]ESRI ArcGIS Software: https://www.esri.com/en-us/arcgis/about-arcgis/overview
[4]HAWQS Software: https://hawqs.tamu.edu/

feature of SWAT is the watershed delineation process — initially, a watershed is subdivided into many subbasins, taking boundaries into consideration based on the surface topology and river network presented [72]. This essentially connects the inlet of one subbasin directly to the outlet of another across the entire watershed [72]. Each of these subbasins is comprised of at least one HRU, one tributary channel, and one main channel, and may also contain impoundments as detailed by the various input data [72]. The various environmental processes are simulated independently at the HRU-level (i.e., no interactions between HRUs are facilitated — any and all spatial relationships are saved for the larger subbasin-level) [72]. While there are numerous equations describing these processes, the fundamental driving force is the water balance equation, used for quantifying the processes exemplified by the hydrologic cycle (i.e., the cyclical, continuous movement of water throughout Earth's various ecosystems, see Figure 3.1 for more information), described below [71]:

$$SW_t = SW_0 + \sum_{i=1}^{t}(R_i - Q_{surf,i} - E_i - P_i - Q_{ret,i}) \tag{3.1}$$

Where i and t refer to time (in days), with i specifically being the summation incremental unit; SW refers to soil water content (mm), with SW_0 being the initial value; R refers to precipitation amount (mm); Q_{surf} refers to surface runoff amount (mm); E refers to evapotranspiration amount (mm); P refers to percolation amount (mm); and Q_{ret} refers to return flow amount (mm).

As HAWQS streamlines SWAT model simulations, the specific details regarding input data can be vastly simplified into selecting the period of analysis, temporal scale (i.e., daily, monthly, or yearly), and weather/climate dataset [71, 72, 75]. Additionally, many input variables, which are automatically initialized, can be customized to accurately describe the region in question per the user's particular needs, such as altering the management practices, point and nonpoint source inputs, sediment routing, and climate sensitivity, among numerous others [75]. Typically, these variables are adjusted in order to calibrate the model (i.e., verify the model outputs correspond well to historical observations across a specific period of time); however, HAWQS has already been calibrated for streamflow, total suspended solids (i.e., sediment), and water quality (e.g., nitrogen and phosphorus), in that specific order,

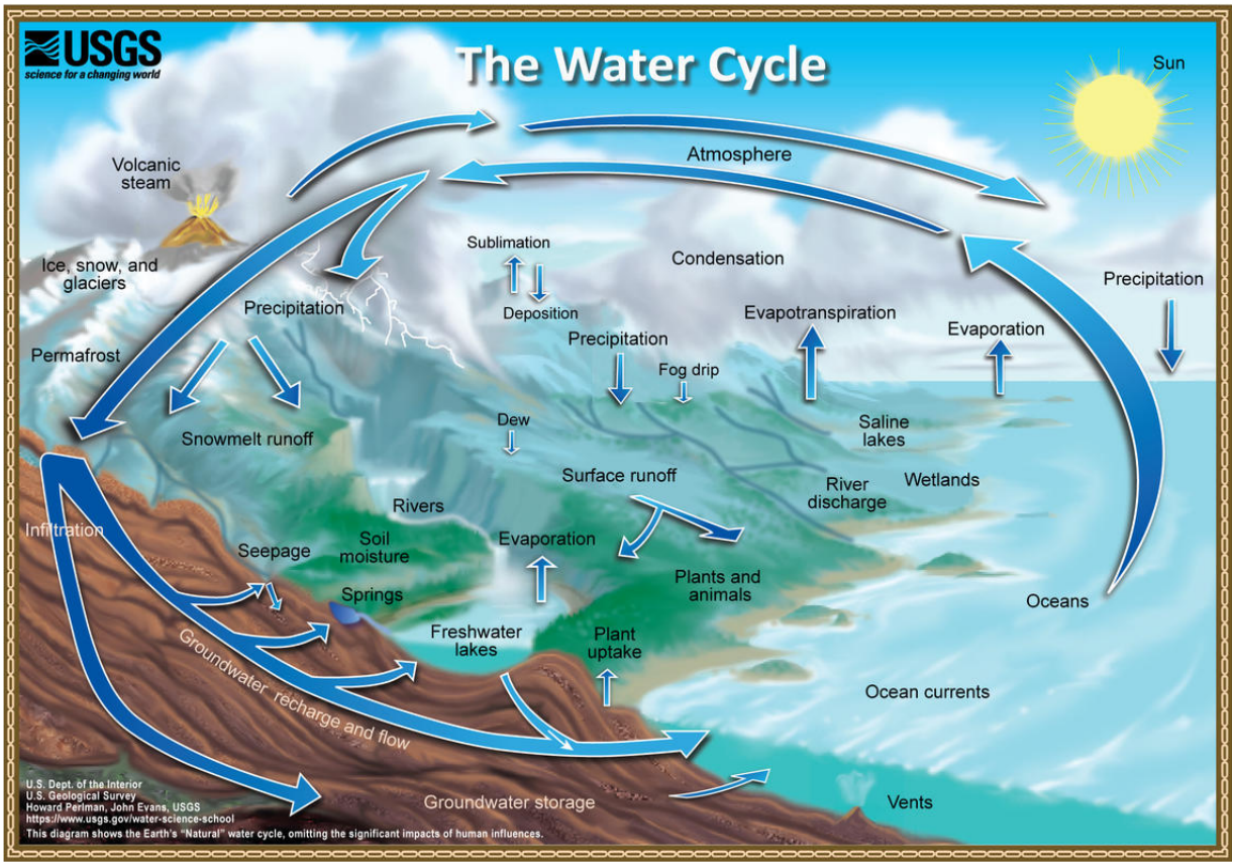

Figure 3.1: Illustration of the Earth's Water Cycle (also referred to as the Hydrologic Cycle) [7].

on a monthly timestep using historical data at the HUC-08 level (per its initial development process) [8]. Specifically, this has been performed for 79 outlet and 570 upstream basins, totaling 30% of continental U.S. HUC-08 watersheds, as illustrated in Figure 3.2 [8]. The resulting parameters were then mapped to the remaining HUC-08 watersheds via a ratio of the HAWQS drainage area to the USGS observed drainage area, and downscaled to the corresponding HUC-10 and HUC-12 watersheds [8].

Accordingly, while some of the details regarding the input data can be overlooked due to the existing calibration process (dependent on the area of interest, as this may not be optimal for certain areas such as the Panhandle of Texas or Montana, per Figure 3.2), understanding how to parse the numerous output data files is still paramount. In particular, the most important output files for most users are the subbasin, main channel, and HRU output files, identified sensibly as *output.sub*, *output.rch*, and *output.hru* [72]. For the subbasin and HRU files, measurements regarding weather conditions (e.g., precipitation, solar irradiation, min and max air temperature, etc.), evapotranspiration, percolation, and total water yield (which comprises contributions to streamflow from surface runoff, groundwater, lateral flow, transmission losses, and pond abstractions), among many others, are contained for each unit within the subbasin- and HRU-levels, along with the unit's identifying information [72]. The main channel file, which refers to how water is routed throughout the watershed between the subbasins (also referred to as reaches within this file), contains time-based measurements related to the average daily rate of flow into and out of the subbasin, evaporation and transmission losses, and identifying information for each subbasin (e.g., code and contributing drainage area), plus many more [72]. Variables important to water quality studies (i.e., those related to sediment and contaminant loadings), are also included in each of these files [72].

HAWQS facilitates simulations based on four historical and 12 climate change weather datasets, and in order to select the most appropriate dataset(s) for our analysis, some additional literature review and modeling trial-runs were necessary [74]. Of the former, which consists of NCDC NWS/NOAA, PRISM, and NEXRAD, both original and bias-corrected, PRISM seemed to show satisfactory correlations with observed records, even under extreme weather conditions [76, 77]. Additionally, PRISM data was available for all of our watersheds, unlike NCDC NWS/NOAA (i.e., this dataset induced errors in simulations of a few

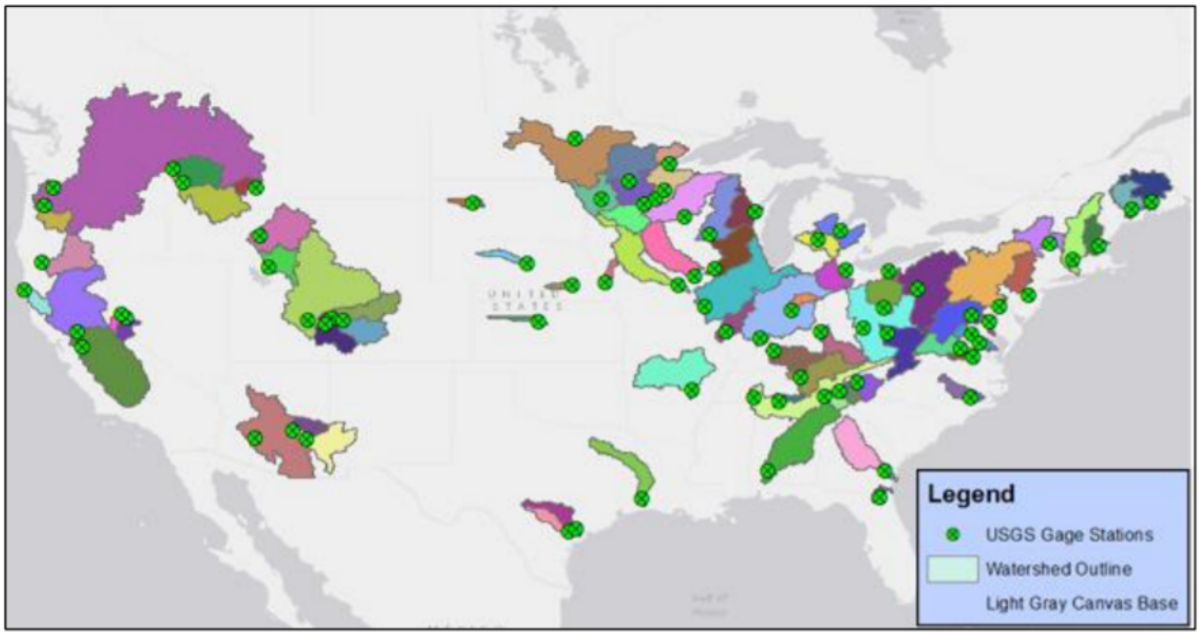

Figure 3.2: Illustration of the currently calibrated HUC-08 regions of the U.S. included in the HAWQS model [8].

watersheds). As for the latter, the included datasets are: ACCESS 1.3, CanESM2, CCSM4, GFDL-CM3, GISS-E2-R, HadGEM2-C, HadGEM2-ES, IPSL-CM5A-LR, IPSL-CM5A-MR, MIROC5, MIROC-ESM-CHEM, and MRI-CGCM3 [74]. All of these are contained within the Coupled Model Intercomparison Project Phase 5 (CMIP5), and mostly differ in terms of resolution and complexity of environmental processes typically included in the Atmosphere-Ocean General Circulation Models (AOGCMs) and broader Earth Systems Models (ESMs), as shown in Figure 3.3. When employing these models, researchers have used anywhere from one to over 18 to analyze the variability of results between each, in an effort to understand the range of potential impacts of climate change on their specific regions of study (usually in terms of streamflow, but also broader hydrology impacts) [39, 47, 78, 79]. Across these analyses, when also incorporated into the SWAT model, CanESM2 and HadGEM2-ES appeared to result in the best baseline correlations with historical datasets (i.e., there was sufficient overlap between model results and historical data for a specific period of time prior to the modeling of future projections) [39, 47, 78, 79]. Per Figure 3.3, HadGEM2-ES is one of the few with the most comprehensive array of environmental processes contained within.

The historical weather data were available from 1 January 1961 (or 1981, depending on the dataset) to 31 December 2018, and the climate change data from 1 January 2006 to 31 December 2099 for two Representative Concentration Pathways (RCPs), 4.5 and 8.5. Generally, the RCP scenarios represent a range of probable climate change mitigation policies and their impacts during the 21st century, organized into four main categories: 2.6, 4.5, 6.0, and 8.5 [9, 45]. RCP 2.6 is considered the best possible case, where radiative forcing both peaks and declines by 2100, and is characterized by extensive policies aimed at reducing greenhouse gas emissions and incorporating cleaner energy resources (for both the power and transportation sectors) [9, 45]. On the other hand, RCP 8.5 is the worst possible case, indicating minimal efforts to reducing emissions and thereby, inducing maximal climate change [9, 45]. RCP 4.5 and 6.0 are incremental cases between these two extremes. Furthermore, both RCP 6.0 and 8.5 showcase the peak of radiative forcing occurring far beyond 2100, while RCP 4.5 has a peak and stabilization (not a declination like 2.6) by 2100 [9, 45]. Each scenario was calculated using a variety of climate models, both AOGCM and ESM, and historic datasets, and provide a comprehensive, but not exhaustive range

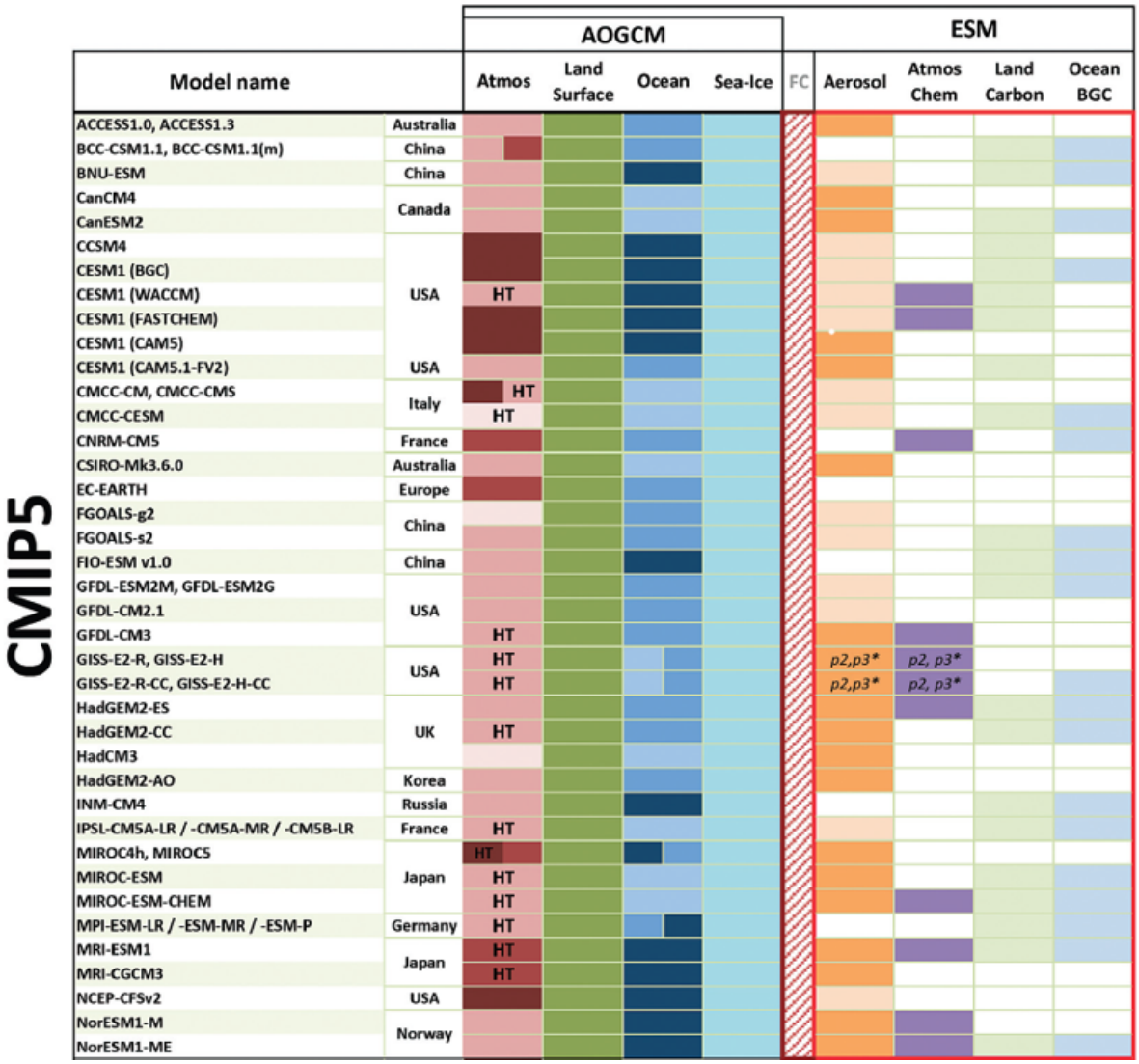

Figure 3.3: Comparison of the numerous Coupled Model Intercomparison Project Phase 5 (CMIP5) climate models, with respect to the important environmental processes of the Atmosphere-Ocean General Circulation Models (AOGCMs) and broader Earth Systems Models (ESMs) [9]. Note that HT refers to high-top atmosphere (i.e., fully modeled stratosphere above stratopause) and darker colors indicate increasing complexity/resolution.

of the possible impacts of climate change incorporating various human actions [9, 45].

3.2 HAWQS Model Setup

Considering PJM's hydropower fleet as discussed in Section 2.3.1, only the 103 HYC plants (recall that RoR and HYC were collectively referred to as HYC due to categorization concerns) were opted for consideration in our analysis — PSH plants were excluded due to their fundamental water transfer functionality (i.e., water is exchanged between reservoirs, indicating that drought and climate change impacts are likely minimal beyond evapotranspiration). Additionally, PSH plants have been excluded from the analyses conducted in similar projects [10, 11, 16, 17, 23, 25, 27, 30, 36, 43]. This set of hydropower plants, along with their corresponding HUC-08 regions (which are necessary for incorporation into HAWQS), have been illustrated in Figure 3.4. These 52 HUC-08 subbasins were simulated using 16 HAWQS models, indicating that not every subbasin required individual modeling due to the water routing nature of the particular watershed in question (e.g., one subbasin can be the outlet for ten upstream subbasins, or have no upstream subbasins at all). To reduce computational burden, small HRUs (i.e., those with areas below $0.25 km^2$) in every subbasin were removed and the remaining HRUs were redistributed to account for this removal [40, 47, 69, 71].

Comparing Figures 3.2 and 3.4, significant overlap is apparent, indicating that a large majority of the PJM region has already been calibrated at the HUC-08 level (on a monthly timestep). Since the more questionable areas are extremely close to the calibrated regions, it is safe to assume that the PJM region as a whole can be assumed to be calibrated as is. Additionally, even though calibration was performed at the monthly timestep, daily was chosen for this analysis to better capture the variability in weather conditions that often occurs on a sub-hourly scale. This will provide more precision and accuracy in our results, especially considering that similar studies in literature were commonly conducted on monthly or annual timescales (however, some were conducted utilizing daily data) [10, 11, 16, 17, 23, 25, 27, 30, 36, 43].

Taking into consideration the array of output files produced by HAWQS (per the

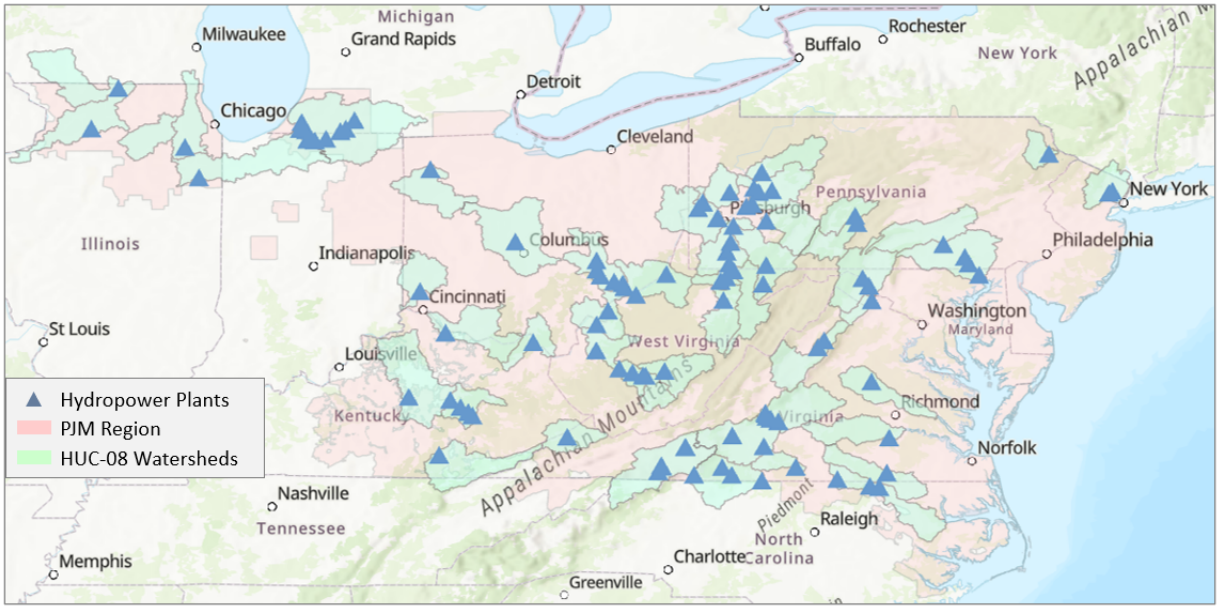

Figure 3.4: Map of PJM's 2030 Hydropower Fleet and their corresponding HUC-08 watersheds.

discussion in Section 3.1.1), information regarding streamflow will be obtained from the *output.rch* file in the form of the *FLOW_IN* and *FLOW_OUT* variables (outputted in units of *cms*), which correspond to the daily average flow into and out of the subbasin. The average of these two variables will be used for each hydropower plant in the subbasin to account for the variability in location and number of hydropower plants across the subbasin, based on the assumption that each plant must pass this specific flow everyday (i.e., no interday storage beyond what was already included in HAWQS, which ensures consistency between steps of the modeling process). Note that accounting for interday storage would require adjustments to be made to our HAWQS models in terms of downstream water routing and various other environmental processes, which was determined to be more prohibitive than beneficial. Using the available datasets and noting the functionality of HAWQS, one historical baseline and nine drought and climate change scenarios were selected: *Historical Normal*, *Historical Drought*, *Moderate Climate Change*, *Moderate Climate Change – Drought*, *Moderate Climate Change – Temperature Drought*, *Moderate Climate Change – Precipitation Drought*, *Severe Climate Change*, *Severe Climate Change – Drought*, *Severe Climate Change – Temperature Drought*, and *Severe Climate Change – Precipitation Drought*. Note that since our hydropower fleet is of 2030, all of these scenarios can be treated as potential projections for the year 2030.

The two historical scenarios comprise years 2011 and 2007, respectively, which were determined by referencing NIDIS DEWS information and comparing the average summer streamflow across each of the plants and using the most typical (i.e., median flow) and drought-like (i.e., lowest flow) years, respectively. Note that this inherently produces some variability, as this does not mean every hydro plant in PJM is undergoing drought or abnormal conditions every day during the summer, only that most are on average experiencing these conditions. On the other hand, the climate change scenarios refer to year 2030 subject to RCP 4.5 and 8.5 influence (i.e., the moderate and severe cases, respectively). Analyzing both available RCPs allows for a more comprehensive understanding of the potential impacts of climate change on a short-to-mid term basis, where there is low probability of significant changes to the existing hydropower fleet beyond what has been expressed in the EIA data. Beyond RCP, these scenarios are further characterized by the

type of drought applied to all subbasins across the summer months (i.e., June–September) — temperature drought (where the air temperature was increased by 2℃), precipitation drought (which faced a reduction of 20%), or both (referred to solely as drought). These values were chosen in light of previous literature studies, which have observed historical droughts exhibiting anywhere from a minor to major deviation in air temperature (i.e., 0.5℃ to 2.0℃ and above increase) and precipitation (i.e., 10% to 60% reduction) [11, 27, 29, 30]. Accordingly, these values, when adjusted for expectations of climate change deviations, represent a severe drought case (i.e., a moderate drought on top of climate change). Each HUC-08 watershed will exhibit nine HAWQS model runs to reflect these scenarios, specifically one historical and eight climate change, where the historical scenario utilizes PRISM data from from 1 January 2000 to 31 December 2018 and the climate change scenarios utilize HadGEM2-ES from 1 January 2020 to 31 December 2030. All runs will utilize five warm-up years (where the model hides output results), which is within the acceptable period of one to ten years according to previous studies and SWAT User Groups[5] [40, 47, 80, 81, 82, 83, 84]. These details for each scenario are summarized in Table 3.1.

3.3 Results of HAWQS Modeling

Per the modeling setup discussed in Section 3.2, involving 103 hydro plants spread across 52 subbasins, we observed significant differences in daily average streamflow among the ten scenarios, albeit with only slight variations in timing and magnitude among the subbasins within each scenario. Since the average of flow into and out of the subbasin was used for each enclosed plant, we can simply analyze the flow regime of each subbasin as a whole instead of for each plant across every scenario. Accordingly, a summary of the major results and trends from this analysis will be presented here. Specifically, the historical flow regime will be compared across a subset of subbasins and the climate change scenarios will be directly compared to the historical flow regime of a single subbasin — these visualizations were chosen in order to best characterize the wider range of trends observed across all subbasins and scenarios (totaling 520 cases).

[5]SWAT User Group: https://groups.google.com/g/swatuser

Table 3.1: Summary of Drought and Climate Change Scenarios.

	Historical – Normal	Historical – Drought	Moderate/ Severe Climate Change	Climate Change – Precipitation Drought	Climate Change – Temperature Drought	Climate Change – Drought
Weather Dataset	PRISM	PRISM	HadGEM2-ES	HadGEM2-ES	HadGEM2-ES	HadGEM2-ES
Start Date	1 January 2000	1 January 2000	1 January 2020	1 January 2020	1 January 2020	1 January 2020
End Date	31 December 2018	31 December 2018	31 December 2030	31 December 2030	31 December 2030	31 December 2030
Reference Year	2011	2007	2030	2030	2030	2030
Number of Warm-Up Years	5	5	5	5	5	5
Timestep	Daily	Daily	Daily	Daily	Daily	Daily
Climate Change Scenario	N/A	N/A	RCP 4.5/8.5	RCP 4.5/8.5	RCP 4.5/8.5	RCP 4.5/8.5
Notes	N/A	N/A	N/A	Summer months are 20% drier	Summer months are 2°C warmer	Summer months are 20% drier and 2°C warmer

Accordingly, Figure 3.5 presents the flow regimes of four subbasins under historical conditions (i.e., 05090201, 02050305, 02080106, and 05050001). Recall that the historical scenarios were modeled across 1 January 2005 to 31 December 2018, and the normal year was defined as 2011 and drought as 2007. These subbasins were chosen to best illustrate the diversity of flow magnitude and timing across the various watersheds in PJM. For these specific subbasins, several key inferences can be made — the former two are much larger than the latter (and also have larger ranges of flow), and all tend to experience lower flows during autumn and higher flows in the winter-to-spring time frame (although this isn't necessarily the case for every year). Generally, this trend of winter/spring peak flow and autumn low flow is apparent across many PJM watersheds, largely due to their proximity and thereby, similar weather and climate characteristics (i.e., as discussed in Section 2.3.2). Note that this trend was also verified with several USGS streamflow gages located throughout the region, referencing the USGS NWIS Database discussed in Section 3.1 [85]. Additionally, the breadth of flow magnitudes found in our results corresponds to the variation in river sizes of our watershed (e.g., larger hydro plants will typically be located on larger river systems, such as downstream of a multi-river confluence).

On the other hand, Figure 3.6 and 3.7 illustrate the general differences between the various moderate and severe climate change scenarios, respectively. Specifically, subbasin 05090201 was selected for this visualization, whose historical flow regime is conveniently contained in Figure 3.5 (top-left corner). Much like the historical scenarios, each of the climate change scenarios tend to follow a trend of high flows in winter/spring and low flows in autumn; however, the relative magnitudes tend to be lower than those of the historical scenarios. Furthermore, the magnitude of the flow regime decreases as the drought conditions become more severe (which was expected for the climate change scenarios) — normal has the largest, followed closely by temperature, and lastly the precipitation and combined drought scenarios. Interestingly, the moderate scenarios exhibit more extreme reductions in flow, but per the discussion of Section 2.3.2, climate change in this region is associated with increased precipitation overall, so these results at least correlate with expectations from literature. Additionally, there are differences in the annual timing of peak and minimum flows between the moderate and severe climate change scenarios, illustrating the variability in weather

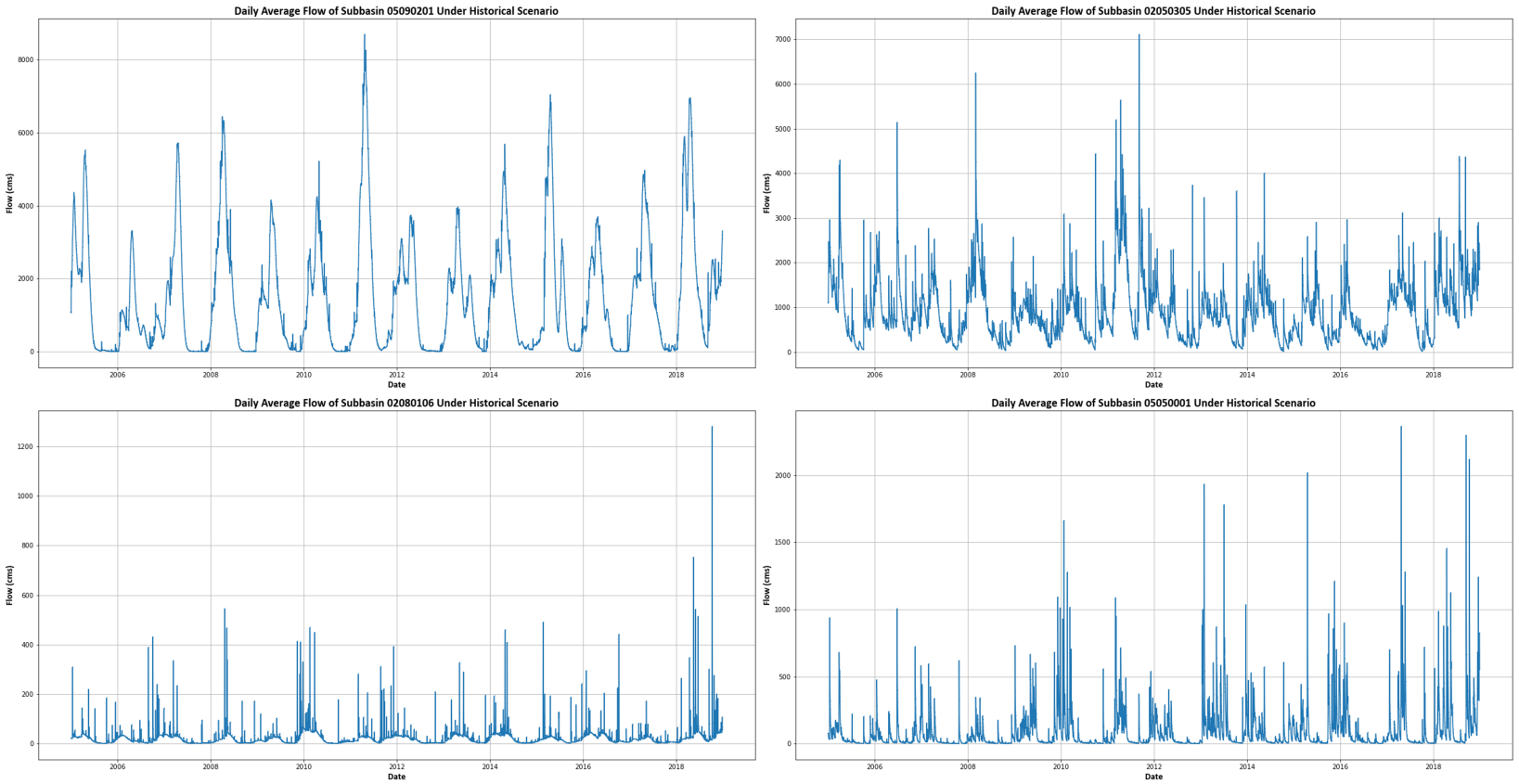

Figure 3.5: General trends of the historical flow regime across a subset of subbasins. Note that the *Historical Normal* and *Historical Drought* scenario years were 2011 and 2007, respectively.

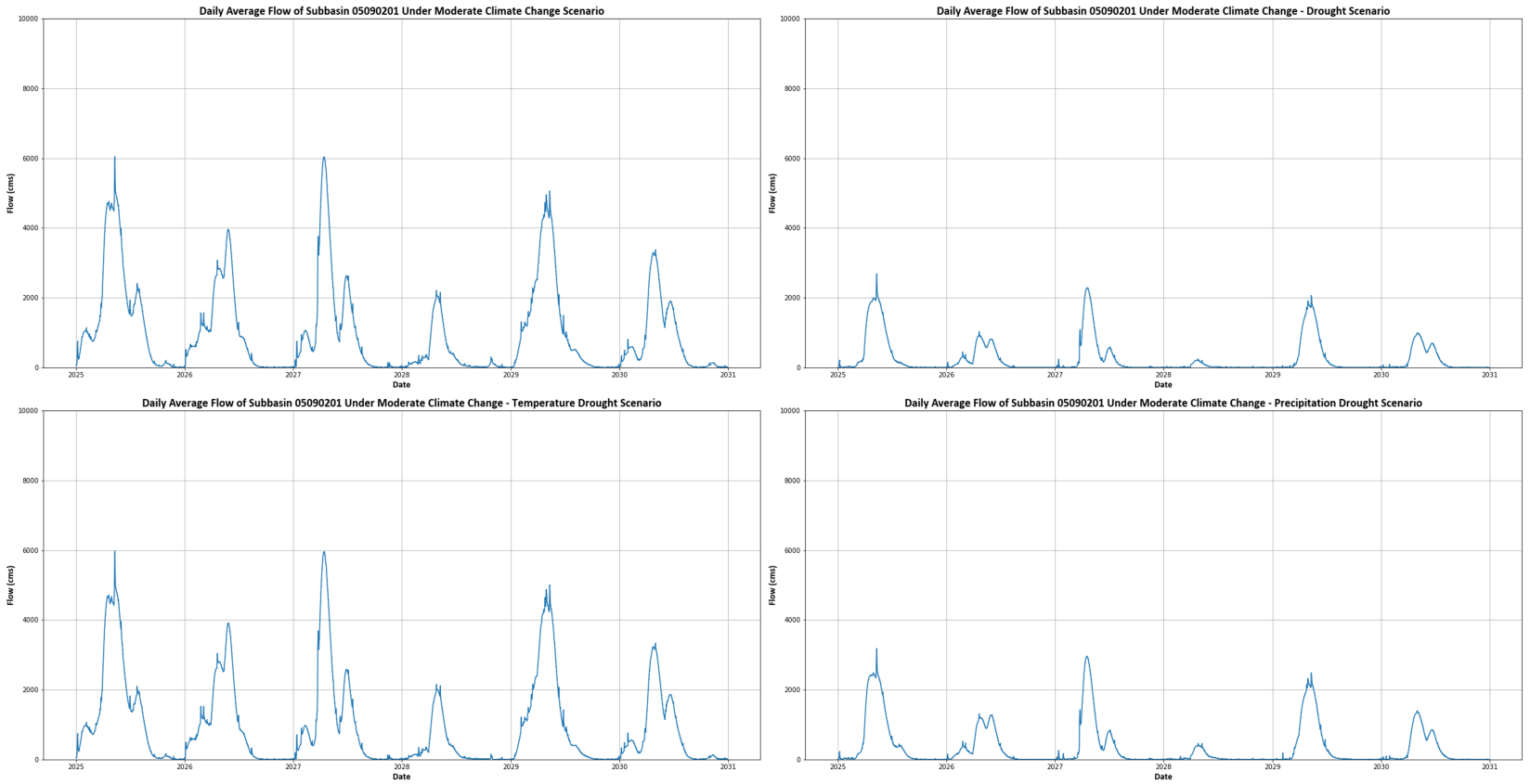

Figure 3.6: General trends of the hydrologic modeling results for the moderate climate change scenarios, of which the year 2030 was selected for further analysis.

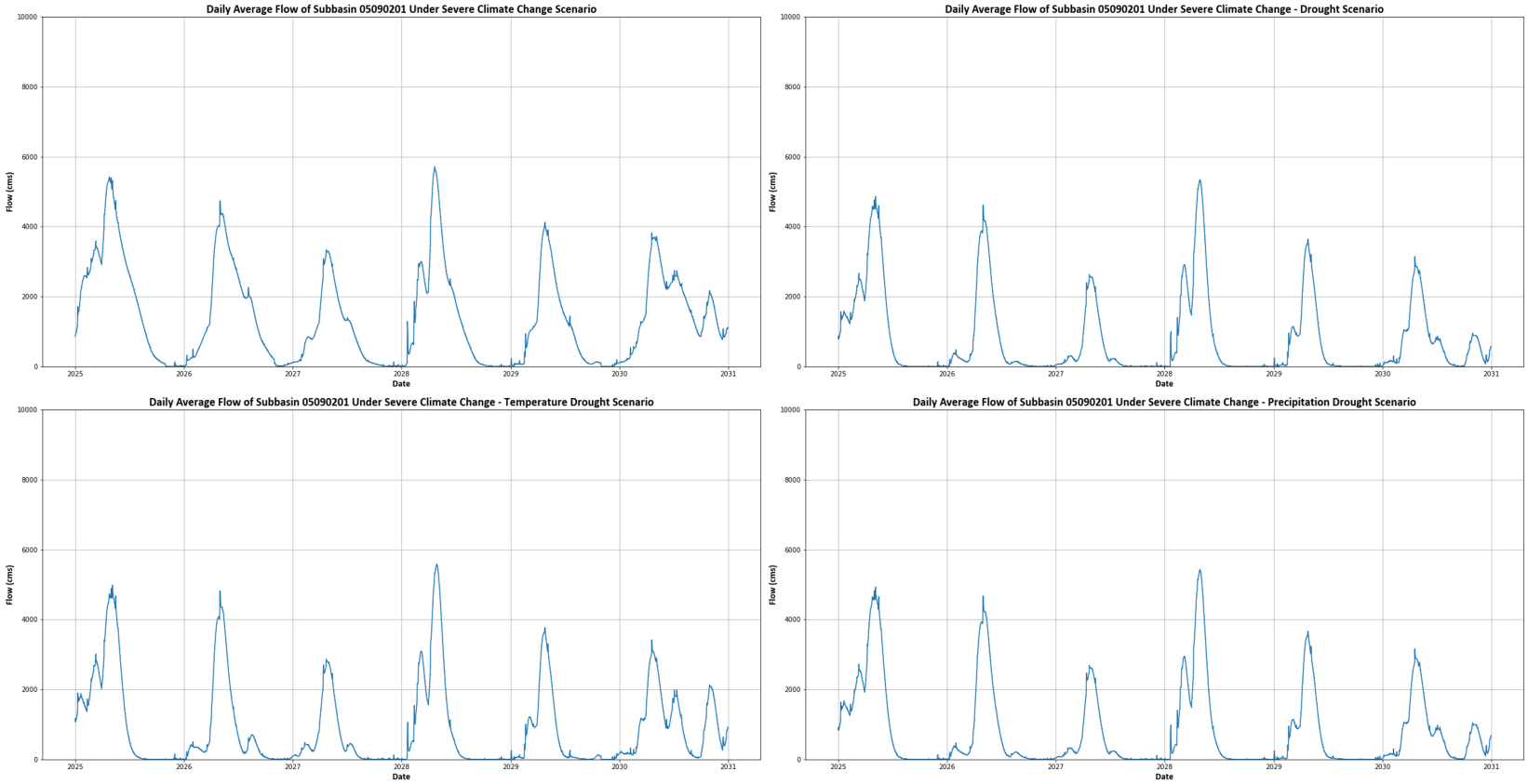

Figure 3.7: General trends of the hydrologic modeling results for the severe climate change scenarios, of which the year 2030 was selected for further analysis.

conditions inherently caused by climate change and appropriately captured in the model. For this specific subbasin, the *Moderate Climate Change – Drought* scenario appears to have the smallest flow regime when compared to the historical and other climate change scenarios; however, this trend isn't readily apparent in every other subbasin and should thereby be treated as an uncommon occurrence.

When isolating the summer months (i.e., June–September) of the specific year used for our analysis (i.e., 2011 for *Historical Normal*, 2007 for *Historical Drought*, and 2030 for the eight climate change scenarios), the general trend is the *Historical Drought* scenario having the smallest flow regime, indicating that this can be treated as a standard for extreme drought conditions (on average). This is also ascertained when comparing each scenario in terms of daily average flow across the entire summer, as presented in Table 3.2. Here, the *Historical Drought* scenario has the absolute lowest average flow, the moderate climate change scenarios have lower average flows than the severe climate change, and the *Severe Climate Change* and *Severe Climate Change – Temperature Drought* scenarios have greater average flows than the *Historical Normal* scenario. Accordingly, the overall impact of climate change on the hydrology of the PJM region encompasses a wide range of possibilities, but is contained within the historical flow regime. However, even though the combined drought cases of the climate change scenarios are not worse than the *Historical Drought* scenario, normal flow conditions have the potential to be lower or higher than what has historically occurred on average. This, in turn, can constrain or expand typical operating schemes, for both hydro and other plants not addressed in our analysis.

Table 3.2: Summary of Summer Daily Average Flow for the Drought and Climate Change Scenarios.

Scenario	Summer Daily Average Flow (cms)	Scenario	Summer Daily Average Flow (cms)
Historical Normal	4,430	**Historical Drought**	1,431
Moderate Climate Change	3,632	**Severe Climate Change**	7,571
Moderate Climate Change – Temperature Drought	3,556	**Severe Climate Change – Temperature Drought**	4,852
Moderate Climate Change – Precipitation Drought	2,126	**Severe Climate Change – Precipitation Drought**	2,873
Moderate Climate Change – Drought	2,000	**Severe Climate Change – Drought**	2,673

Chapter 4

Impact Modeling

From the discussion in Chapter 3, the main output of the hydrologic modeling process is a daily average streamflow value for each hydropower plant across all scenarios (i.e., *Historical Normal*, *Historical Drought*, *Moderate Climate Change*, *Moderate Climate Change – Drought*, *Moderate Climate Change – Temperature Drought*, *Moderate Climate Change – Precipitation Drought*, *Severe Climate Change*, *Severe Climate Change – Drought*, *Severe Climate Change – Temperature Drought*, and *Severe Climate Change – Precipitation Drought*). This streamflow value will then be translated into specific impacts spanning the individual hydropower plant, larger hydropower fleet, and broader PJM power system. Accordingly, this chapter gives an overview of this process, encompassing:

- Modeling of generation impacts (Section 4.1);
- Modeling of economic impacts (Section 4.2); and
- Modeling of reliability impacts (Section 4.3).

4.1 Generation Modeling

Unlike thermal power plants, which tend to power-constrained in the sense that the immediate water conditions (i.e., both availability and quality) have a direct impact on the power capacity available (i.e., the potential for the maximum capacity available to

be less than the plant's installed capacity), hydropower plants tend to be more energy-constrained due to most plants relying on water stored in sizable reservoirs to produce power [1, 10, 11, 16, 17, 19, 24, 25, 37, 36, 42, 49]. This allows for the effects of short-term droughts to be effectively minimized since enough energy is stored for multiple generation periods, which can comprise days, weeks, and even months, depending on the particular operational scheme employed (i.e., how many hours at what capacity is the plant dispatched) [1, 10, 11, 16, 17, 19, 24, 25, 36, 49]. Therefore, even without a resupply of water for an extended period of time, the impacts of drought conditions on hydropower plants may not always be immediately realized, and rather only appear after several weeks or more [1, 10, 11, 16, 17, 19, 24, 25, 36, 49]. However, many (if not all) hydropower facilities have specific requirements for maintaining environmental flows (also commonly referred to as minimum flows) through the facility, sometimes even with quality requirements (e.g., water temperature, nutrient concentration, etc.) [86, 87]. These flows serve to maintain the river ecosystem, whether for purely environmental reasons (e.g., endangered species) or some economic purpose (e.g., to preserve downstream sporting fisheries), and can come in the form of hourly, daily, or weekly commitments [86, 87]. For instance, a plant could be required to maintain a $3cms$ daily average flow rate out of the facility, but is free to decide how exactly to reach that target, meaning they could time outflows with generation periods, per the dispatch schedule, to maximize revenue and still fulfill the requirement (otherwise, this water would need to be passed without generating, representing a loss of revenue for the owner/operator) [86].

Taking this information into consideration, the daily average streamflow (outputted by HAWQS and translated to each individual plant) will be converted into a daily total streamflow value (i.e., the total volume of water moved that day, ignoring any interday storage contributions), which will then be used to determine how many hours the plant could generate at its installed or nameplate capacity (i.e., maximum power output), ultimately resulting in a total daily generation value. This procedure was selected in order to streamline and simplify modeling efforts. For instance, power plants can have a multitude of turbine-generators comprising their installed capacity, allowing generation at varying levels for different lengths of time [62, 86, 87]. While this feature is invaluable for unit commitment

studies, the overarching goal of our analysis is to broadly understand the potential impacts of drought and climate change on hydropower resources and broader grid reliability, specifically by staying in the generation realm of the power system (i.e., unit commitment would move beyond generation by also involving the transmission and distribution aspects). Therefore, focusing on generation at capacity ensures that the maximum possible amount of power will be produced each day, given the constraint of our procedure assuming that the streamflow outputs from HAWQS must be passed each day as shown.

Accordingly, to calculate total daily generation, two main equations are utilized — one for calculating the design flow corresponding to the plant's installed capacity, and another where that value is then combined with daily average streamflow. The design flow is obtained using a modified version of the standard hydroelectric power equation [17, 25]:

$$Q_{design} = \frac{P_{cap} \cdot 10^6}{H \cdot \rho \cdot g \cdot \eta} \tag{4.1}$$

Where Q_{design} refers to the design flow of the plant (cms); P_{cap} refers to the installed capacity of the plant (MW), with a conversion factor from MW to W; H refers to hydraulic head of the plant (m); g refers to the gravitational acceleration constant (9.8 m/s^2); ρ refers to the density of freshwater (1,000 kg/m^2); and η refers to plant efficiency, which comprises power losses from operation of the turbine-generators (%). Installed capacity was obtained from the EIA and ORNL databases, and plant efficiency was assumed to be 90%, according to typical literature assumptions [25, 61, 62]. On the other hand, data regarding hydraulic head was obtained by multiplying the plant's dam height by a 0.8 factor, based on the assumption that dam height overestimates hydraulic head for most plants, which tend to have the powerhouse located immediately downstream of the dam [2, 17, 35, 37]. However, this is not true for all plants, as some have the powerhouse located many miles downstream, thereby insinuating that this value can be an underestimation [2, 17, 35, 37]. Regardless, this factor is used per guidance of best practices according to literature, noting that some studies have shown that variation and/or uncertainties in hydraulic head had minimal effects on resulting power values, or usable capacity, of hydropower plants [17]. Dam height data

for each plant was obtained from the USACE National Inventory of Dams (NID) Database[1], encompassing multiple values obtained from different sources [88]. Accordingly, the NID preferred value was used in this analysis, which is the maximum value among the available dam heights [88].

The next step is to combine this resulting design flow with the daily average streamflow, outputted from the HAWQS simulations, to ascertain the plant's total daily generation via:

$$P_{day,total} = P_{cap} \cdot \frac{Q_{day,avg} \cdot 86,400}{Q_{design} \cdot 3,600} \tag{4.2}$$

Where $P_{day,total}$ refers to the plant's total daily generation (MWh); $Q_{day,avg}$ refers to the daily average streamflow outputted for the plant (cms), with a conversion factor from cms to cmd; and Q_{design} refers to the design flow for the plant obtained in Equation 4.1 (cms), with a conversion factor from cms to cmh. Resulting from the combined usage of Equations 4.1 and 4.2, each plant will have a total daily generation value for every day of the four scenarios. Recall that our analysis is primarily concerned with the summer months (i.e., June–September) so values from the rest of the year will be ignored.

4.1.1 Results

In order to best characterize our generation results in the context of the goals of our analysis, the drought and climate change scenarios will be discussed relative to the *Historical Normal* scenario. Therefore, one additional formula will be required to present these results, percent change, expressed via [89]:

$$\%\Delta = \frac{P_{hist} - P_{new}}{P_{hist}} \cdot 100\% \tag{4.3}$$

Where P_{hist} refers to the total daily generation of the *Historical Normal* scenario (MWh); P_{new} refers to the total daily generation of the drought and/or climate change scenario (MWh); and $\%\Delta$ refers to percent change (%). Additionally, to account for inter-daily variability between scenarios (i.e., in terms of weather trends and patterns), monthly summations of total daily generation will be utilized. Accordingly, we can then quantify

[1]USACE NID Database: https://nid.sec.usace.army.mil/#/

potentially problematic months, scenarios, and hydro plants, which would then indicate areas requiring more analysis to best understand and characterize the extent of the vulnerabilities.

Table 4.1 presents the monthly summations of total daily generation for each scenario and the percent change relative to the *Historical Normal* scenario. Here, several key inferences can be made — namely, the *Historical Drought* scenario has the overall worst-case impact on hydropower generation; however, on a monthly basis, more fluctuations between scenarios is apparent, illustrating some of the variability imposed by climate change. For instance, the *Historical Normal* scenario has August as the lowest generation month (this was a significant decrease relative to the surrounding months), which is only reflected in the precipitation and combined drought cases of severe climate change. The rest, except for the *Historical Drought* scenario, have consistent decreases throughout the summer (i.e., where June has the highest and September has the lowest). This is most likely due to the compounding drought events imposed by the HAWQS model (i.e., the drought conditions were imposed consistently across the entire summer and thereby, would continually increase in severity with only slight respite within the period), whereas historically what is considered a summer-wide drought can have various weeks of non-drought conditions.

Another interesting result are the instances (i.e., scenarios and months) where total generation increased relative to the *Historical Normal* scenario. Specifically, overall the *Severe Climate Change* scenario had a significant increase, resulting from ascending gains in the months of June, July, and August. Also note that the latter had the largest absolute value across all instances with an 173.8% increase (the runner-up only reached 94.1% decreasingly). The *Severe Climate Change - Temperature Drought* scenario also follows this trend, just not nearly to the same magnitude, as the overall change is nearly zero with a 0.1% decrease. Additionally, the *Moderate Climate Change* and *Moderate Climate Change – Temperature Drought* scenarios also had gains, but only in the months of July and August. Overall, the climate change scenarios can be divided into two groups based on the proximity of their results: the base and temperature drought scenarios and then the precipitation and combined drought scenarios, with the latter having much lower generation results. Compared with Table 3.2, roughly the same general trends can be observed, albeit without the monthly breakdowns.

Table 4.1: Total Monthly Generation Across All Plants in Each Scenario.

Scenario	Total Generation by Month (MWh) Percent Change Relative to Historical Normal				
	June	July	August	September	All
Historical Normal	1,468,520	804,397	367,068	1,103,433	3,743,417
Historical Drought	574,739 (-60.9%)	244,347 (-69.6%)	316,599 (-13.7%)	230,051 (-79.2%)	1,365,737 (-63.5%)
Moderate Climate Change	1,428,692 (-2.7%)	971,388 (+20.8%)	386,650 (+5.3%)	127,717 (-88.4%)	2,914,447 (-22.1%)
Moderate Climate Change – Temperature Drought	1,451,485 (-1.2%)	984,510 (+22.4%)	415,893 (+13.3%)	141,056 (-87.2%)	2,992,944 (-20.0%)
Moderate Climate Change – Precipitation Drought	1,151,019 (-21.6%)	685,080 (-14.8%)	236,646 (-35.5%)	70,672 (-93.6%)	2,143,418 (-42.7%)
Moderate Climate Change – Drought	1,109,131 (-24.5%)	639,266 (-20.5%)	215,121 (-41.4%)	65,039 (-94.4%)	2,028,556 (-45.8%)
Severe Climate Change	1,562,034 (+6.4%)	1,308,039 (+62.6%)	1,004,945 (+173.8%)	973,025 (-11.8%)	4,848,043 (+29.5%)
Severe Climate Change – Temperature Drought	1,489,835 (+1.5%)	1,092,156 (+35.8%)	592,359 (+61.4%)	563,462 (-48.9%)	3,737,812 (-0.1%)
Severe Climate Change – Precipitation Drought	1,269,084 (-13.6%)	781,070 (-2.9%)	280,426 (-23.6%)	316,534 (-71.3%)	2,647,114 (-29.3%)
Severe Climate Change – Drought	1,252,004 (-14.7%)	728,364 (-9.5%)	242,851 (-33.8%)	297,531 (-73.0%)	2,520,750 (-32.7%)

In addition to these generation results, we can ascertain the most vulnerable plants across the fleet with respect to drought and climate change conditions. Table 4.2 summarizes those plants (13 total) where a near complete deration occurred (i.e., approximately a 99–100% decrease relative to the *Historical Normal* scenario). Overall, the most problematic scenarios and month were the precipitation and combined drought cases of moderate climate change in September. Rarely did any plant deviate from this trend — there was one instance each of July, *Historical Drought*, and *Moderate Climate Change*, and two instances of *Moderate Climate Change – Temperature Drought*. As discussed previously, precipitation and combined drought scenarios of climate change are heavily coupled, indicating that by September, these scenarios under moderate climate change conditions are significantly impacting the operation, as well as economic viability, of these hydro plants (note that other plants are also adversely affected during these scenarios, just not quite to this extent). This, in turn, has major implications on the reliability of the broader power system, which will be explored later in Section 4.3. Additionally, many of these identified plants are located in the same HUC-08 subbasin or are apart of the same watershed routing system (per our HAWQS models), implying that the certain regions are more heavily impacted than others, even when subject to the same overall drought conditions. This most likely suggests that localized weather patterns can also play a significant role in determining the extent of drought impacts (however, only slightly as it's doubtful that a subbasin in this region would be experiencing "wet" conditions while its neighbor was in extreme drought).

4.2 Economic Modeling

While the initial capital costs (in $\$/KW$) of hydro tend to be larger than many other types of generation resources, its operational costs are minuscule, rivaled only by wind and solar, largely due to the virtual lack of fuel costs [38]. Therefore, even though it is plausible to replace any lost hydro generation capability with wind and/or solar, these renewables do not exhibit nearly the same level of operational flexibility as hydro (as outlined in Section 2.2.2), at least without considering energy storage technologies (i.e., to compensate for times when weather conditions prohibit generation, e.g., wind speeds too fast or slow, or no

Table 4.2: Hydro Plants Most Vulnerable to Drought and Climate Change Conditions (i.e., those nearly completely derated relative to the *Historical Normal scenario*).

EIA Code	Name	Installed Capacity (MW)	State	HUC-08 Subbasin	Scenario(s)	Month
7128	William F Matson Generating Station	21.7	PA	02050303	Moderate Climate Change - Temperature Drought	September
					Moderate Climate Change - Precipitation Drought	September
					Moderate Climate Change - Drought	September
1574	Conowingo	530.8	MD	02050306	Moderate Climate Change - Precipitation Drought	September
					Moderate Climate Change - Drought	September
3145	Holtwood	247.3	PA	02050306	Moderate Climate Change - Precipitation Drought	September
					Moderate Climate Change - Drought	September
3175	Safe Harbor	417.5	PA	02050306	Moderate Climate Change - Precipitation Drought	September
					Moderate Climate Change - Drought	September
2756	Gaston	177.6	NC	03010106	Historical Drought	September
62384	Point Marion L&D Hydroelectric Project	5	PA	05020003	Moderate Climate Change - Precipitation Drought	September
					Moderate Climate Change - Drought	September
62386	Opekiska L&D Hydroelectric Project	6	WV	05020003	Moderate Climate Change - Precipitation Drought	September
					Moderate Climate Change - Drought	September
62387	Morgantown L&D Hydroelectric Project	5	WV	05020003	Moderate Climate Change - Precipitation Drought	September
					Moderate Climate Change - Drought	September
6636	Lake Lynn Hydro Station	51.2	PA	05020004	Moderate Climate Change	September
					Moderate Climate Change - Temperature Drought	September
					Moderate Climate Change - Precipitation Drought	September
					Moderate Climate Change - Drought	September
50036	New Martinsville Hannibal Hydro	37.4	WV	05030201	Moderate Climate Change - Precipitation Drought	September
					Moderate Climate Change - Drought	September
57401	Willow Island Hydroelectric Plant	44	WV	05030201	Moderate Climate Change - Precipitation Drought	September
					Moderate Climate Change - Drought	September
6006	Racine	47.4	OH	05030202	Moderate Climate Change - Drought	July
4258	Greenup Hydro	70.2	OH	05090103	Moderate Climate Change - Drought	September

sunlight) [5, 38]. Accordingly, for the immediate future, the most likely replacement are natural gas combustion turbines, which can provide nearly identical ancillary grid services in terms of reliability and flexibility (i.e., synchronous and non-synchronous reserve, frequency and voltage regulation, and load-following and black-start capability) [5]. However, fossil fuel-fired plants such as this have nontrivial fuel costs that must be understood when assessing utilization [38].

To best characterize the economic impacts of lost hydro generation in the context of our analysis, the levelized cost of energy (LCOE) for hydro and natural gas combustion turbines will be compared. By definition, LCOE combines both initial capital and operating (both fixed and variable) costs along with transmission costs to ascertain a single value representing that particular energy source [90]. For many technologies, the impacts of subsidies, tax credits, and other incentives can also be included to reflect current market conditions [90]. Per the EIA, the LCOE for hydro is $\$64.27/MWh$ and natural gas combustion turbine is $\$117.86/MWh$ [90]. Note that these values encompasses the entire U.S. as of 2021, but are projected to incorporate resources entering into service by 2027, which corresponds adequately to our analysis year of 2030 [90]. Additionally, the spatial and temporal variability in costs of energy are overlooked in favor of this simplistic LCOE approach to garner a generalized idea of potential economic impacts [36, 90].

4.2.1 Results

As discussed in Section 4.1.1, the *Historical Drought* scenario has the most significant reduction in generation compared to the *Historical Normal* scenario, followed by the combined drought and precipitation cases of the moderate and severe climate change scenarios, respectively. Then, while the base and temperature drought cases of moderate climate climate change still experienced reductions, the severe climate change base case underwent an extreme increase in generation and the temperature drought case barely changed relative to the *Historical Normal* scenario. Accordingly, the expected increases in costs from replacing reduced hydro generation with natural gas combustion turbines follows the same trend, except at a greater order of magnitude due to the corresponding LCOEs, as shown in Table 4.3. Expected replacement costs of the drought and climate change

Table 4.3: Costs of Replacing Lost Hydro Generation with Natural Gas Combustion Turbines due to Drought and Climate Change Conditions (relative to the *Historical Normal* scenario).

Scenario	Difference in Total Generation relative to Historical Normal (MWh)	Costs of Replacement with Natural Gas Combustion Turbines
Historical Normal	N/A	N/A
Historical Drought	-2,377,681	$127,419,921
Moderate Climate Change	-828,970	$44,424,508
Moderate Climate Change – Temperature Drought	-750,473	$40,217,853
Moderate Climate Change – Precipitation Drought	-1,600,000	$85,743,974
Moderate Climate Change – Drought	-1,714,861	$91,899,402
Severe Climate Change	+1,104,626	$59,196,883 (savings)
Severe Climate Change – Temperature Drought	-5,605	$300,386
Severe Climate Change – Precipitation Drought	-1,096,304	$58,750,916
Severe Climate Change – Drought	-1,222,668	$65,522,767

scenarios range from $330 thousand to $127 million for the summer (including a savings of $59 million for the *Severe Climate Change* scenario), which would have significant impacts on plant owner/operator budgets and consumer energy bills. However, note that these figures assume that that all of the hydropower generation is essential to fulfill electricity demand, meaning that every lost MWh must be replaced, which isn't necessarily realistic depending on actual operating conditions.

4.3 Reliability Modeling

Due to the breadth of ancillary grid services provided by hydropower to the wider power system (i.e., making hydro a critical player in ensuring grid reliability and resiliency, as discussed in Chapter 2.2), conditions that threaten to constrain, especially derate, plant operation are important to understand and characterize. Accordingly, numerous metrics have been developed to evaluate the reliability status of the power system under various conditions (e.g., extreme weather, capacity expansion/reduction, load expansion/reduction, etc.), including [91, 92]:

- Loss of Load Probability (LOLP) – refers to the probability of load exceeding available generation capacity (also called Loss of Load Expectation if converted into a $day/year$ unit format).
- Expected Demand Not Supplied (eDNS) – refers to the expected load not met due to insufficient available generation.
- Expected Energy Not Supplied (eENS) – refers to the expected energy difference between available generation and expected load, where the latter exceeds the former.

Per our analysis, we evaluated the potential impacts of various drought and climate change conditions on hydropower generation in 2030. Since hydro was specifically isolated and no other generation resources (e.g., coal, natural gas, nuclear, etc.) were modeled, the LOLP reliability metric is most applicable, as it allows us to simply utilize plant capacities for these generators instead of actual generation values (i.e., energy, which is necessary for calculating eDNS and/or eENS). In reference to the U.S. power system, the typical LOLP

requirement is an insufficient generation capacity outage occurring less than one day in ten years, which has a probability of 0.00027 (or 2.7e-4) [91, 92, 93]. Determining the system's LOLP revolves around the following equation [91, 92]:

$$LOLP = \sum_{i=1}^{t} P_i(C_i < L_i) \tag{4.4}$$

Where i and t refer to time in days, with i specifically being the summation incremental unit; C_i refers to the available capacity (MW); L_i refers to the daily peak load (MW); and $P_i(C_i < L_i)$ refers to the probability of loss of load. Within Equation 4.4, the probabilities of each possible capacity outage are ascertained, which is based on each generator's forced outage rate (FOR), or the probability of generator failure when scheduled to operate, and then the resulting available generation capacity is compared the system's load duration curve (i.e., probabilities of a specific load occurring) [91, 92, 93]. For systems with many generators (such as PJM), this analytical (deterministic) approach is extremely computationally inefficient due to the sheer volume of capacity outage permutations possible — because generators are treated as binary elements (i.e., they can either be online or offline), the total number of permutations are on the order of 2^n, where n is the number of generators. For example, a system with 25 generators has 33,554,432 possible capacity outage combinations. However, note that not all permutations are realistic or even have a worthwhile probability (e.g., all generators being offline would have a negligibly low probability).

Therefore, various stochastic approximation methods can be implemented to overcome these challenges, such as Monte Carlo simulations [92, 93, 94]. For an LOLP-specific application, the determination of the capacity outage permutations can be randomized using Monte Carlo and then repeated to ensure an appropriate accuracy has been been obtained [92, 93, 94]. Monte Carlo iterations are typically performed on the order of one, ten, and one hundred thousand, and one million to test the variability in distribution of resulting values [94]. The final iteration number (i.e., to be used for the rest of the analysis) is then selected by balancing computational time with the utility of the resulting distribution [94].

4.3.1 Additional Detail on LOLP Modeling

Calculating LOLP involves ascertaining two key pieces of data: generation fleet (specifically, the nameplate capacity, fuel type and/or prime mover, location, balancing authority, and FOR of each generator) and electricity demand (on an hourly basis). As discussed in Section 2.3.1, the EIA Form 860 Database contains general information for all generators across the U.S., allowing us to identify and characterize those contained within PJM's territory (note that the term generators refers to individual units, meaning that a particular power plant can be comprised of multiple generators) [62]. Following the procedure for the hydropower fleet during the earlier portion of our analysis (refer to Section 2.3.1), PJM's entire generation fleet will incorporate all currently operational plants, planned retirements, and proposed additional generation to the year 2030 (per 2020 plans). In total, the installed capacity of PJM's generation fleet exceeds $222GW$ spread across 3,720 individual generators.

Regarding the last piece of generator data (i.e., FOR), PJM's Data Miner 2 Database can be utilized, as it contains FORs for various types of generation units on a monthly basis, excluding wind and solar due to their intermittent nature of operation (i.e., they are not on-demand generators) [34, 95]. Note that PJM refers to their FORs as equivalent demand FORs, which is defined as the probability of a generator being forcibly taken of out service during its scheduled operation [34]. Accordingly, since this is not extremely different from our definition of FOR, it will be simply referred to as FOR (also note that FOR does not encompass scheduled outages per these definitions). When including this data in our analysis, the maximum value of the last five years will be utilized to represent a worst-case scenario of FORs in recent history (here, recent is important to ensure that the most modern and up-to-date equipment employed in the generation fleet is characterized). Additionally, to compensate for the exclusion of wind and solar in the PJM FOR data, there are two methods to obtain an approximate FOR value [95]:

1. Capacity Value – calculate how adequately generation aligns with peak demand patterns.

2. Effective Load Carrying Capacity (ELCC) – utilize reliability metrics (e.g., LOLP) to gauge how much load can increase with the inclusion of this renewable generator in the system while maintaining the same level of reliability.

Due to the inclusion of reliability metrics in the procedure of ELCC (whose value was initially planned to be used as a FOR approximation in our broader reliability assessment), the *Capacity Value* method is the more practical option. Accordingly, to calculate the capacity value of wind and solar, their historical generation relative to their installed capacity was compared across an 100-*hour* subset of peak load values for a given year (across the entire PJM region) [95]. Hourly generation and load data for 2021 was utilized and obtained from PJM's database (to represent the most recent annual experience), and the wind and solar fleet as of 2021 was obtained using the EIA database [34, 62]. To approximate FOR, note that capacity value closely resembles availability (AVL) in theory, which is related to FOR via the following equation [91, 92, 93]:

$$1 = FOR + AVL \tag{4.5}$$

Where both FOR and AVL are expressed as percentages in decimal format. Table 4.4 summarizes the FOR and AVL according to PJM's composition scheme of plant types. While the generator data obtained from EIA did not exactly match this scheme, it contained enough descriptive information between the technology and prime mover entries to facilitate appropriate matching between the datasets (e.g., natural gas fired combustion turbine is combustion turbine, natural gas internal combustion engine or natural gas steam turbine is gas, etc.). Additionally, most plants generally have similar FOR values so any inconsistencies should have limited impacts, and these trends generally follow that of PJM official documents [5]. Figure 4.1 illustrates the capacity breakdown of PJM's generators subject to this composition scheme.

As shown in the capacity value calculation, the PJM database can be utilized to obtain the second key piece of data, electricity demand [34]. Similarly, we can take 2021 hourly load data and linearly scale it subject to the forecasted peak summer load of 2030, which can be obtained from PJM's annual load forecast reports [96, 97, 98, 99, 100]. In addition

Table 4.4: Historical Forced Outage Rates for Various Power Plants in PJM.

Plant Type	Forced Outage Rate (%)	Availability (%)
Combined Cycle	3.3715	96.6285
Combustion Turbine	7.2735	92.7265
Diesel	10.4007	89.5992
Gas	19.6377	80.3623
Hydro	6.9725	93.0275
Nuclear	1.80525	98.1947
Oil	26.7390	73.2610
Other	14.0320	85.9680
Pumped Hydro	6.47875	93.5212
Coal <299MW	12.7033	87.2968
Coal 300-599MW	12.1895	87.8105
Coal >600MW	12.1258	87.8743
Wind	84.4726	15.5274
Solar	70.1603	29.8397

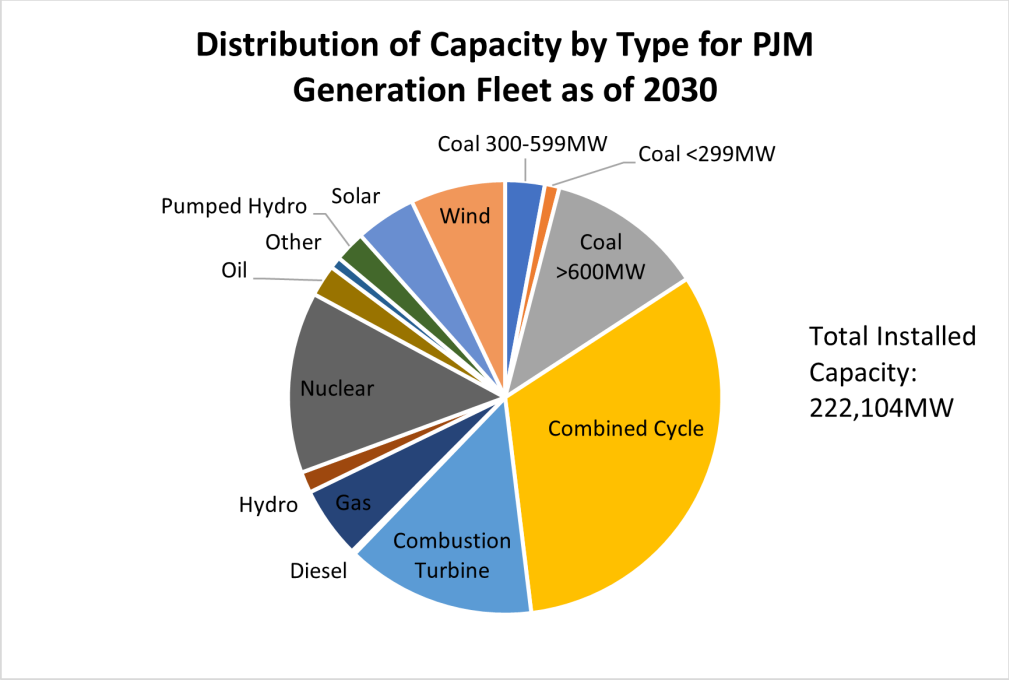

Figure 4.1: Distribution of capacity by type for PJM generation fleet (as of 2030).

to a base forecast of summer load, these reports contain an extreme summer case, which essentially reflects an increase in peak load upwards of $10GW$, allowing us to perform reliability calculations with loading conditions more closely reflecting the scenario employed (i.e., as discussed in Chapter 1 and 2, extreme weather is typically associated with impacts across all parts of the power system, not just generation) [96, 97, 98, 99, 100]. Therefore, the *Historical Normal* scenario will utilize the normal summer case and the remaining drought and climate change scenarios will utilize the extreme summer case [96, 97, 98, 99, 100]. Additionally, while multiple reports across the past decade were reviewed, only the values from the most recent will be utilized (i.e., 2022) — besides this being the most up-to-date report, a trend of major reductions in forecasted summer load was observed across the past decade (e.g., for 2025, the 2010 report forecasted $182GW$ while 2022 forecasted $151GW$), as shown in Table 4.5 [96, 97, 98, 99, 100]. While there can be a multitude of reasons for this substantial difference, the reports mainly cite fundamental changes in modeling techniques along with increases in energy efficiency and changes in consumption patterns (e.g., relocation of industrial users) [96, 97, 98, 99, 100].

To incorporate these two loading conditions into our reliability calculations, they must first be converted into load duration curves, which describe the probability of a particular load occurring [91, 92, 93]. Specifically, these curves are based on daily peak load (i.e., the maximum load hour of each day), instead of all load values throughout the year, to capture the most probable subset of cases where loss of load could be an issue [92, 93]. Figure 4.2 illustrates these load duration curves, which have spans of 75–$154GW$ and 79–$162GW$ for the normal and drought cases, respectively (recall that per our simplifications, the drought case is simply the normal case linearly scaled up).

Now, with the load duration curves, generation fleet, and FOR/AVL of all generators in PJM, we can perform our Monte Carlo-based LOLP calculations. The *Historical Normal* scenario will utilize these base FOR/AVL values while each subsequent drought and climate change scenario will have an adjusted FOR/AVL value (for hydro only) based on the change in generation relative to the *Historical Normal* scenario. This will simply be reflected via a linearly proportional scaling, i.e.:

Table 4.5: Metered and Expected (normal) Summer Peak Loads from Various PJM Load Forecast Reports.

Load Forecast Report	Metered Summer Peak Load (GW)	Expected Summer Peak Load (GW)			
	Year Before	2020	2025	2030	2035
2010	(2009) 127	174	182	-	-
2015	(2014) 141	164	172	178	-
2020	(2019) 151	148	153	157	160
2021	(2020) 144	-	152	153	154
2022	(2021) 148	-	151	154	156

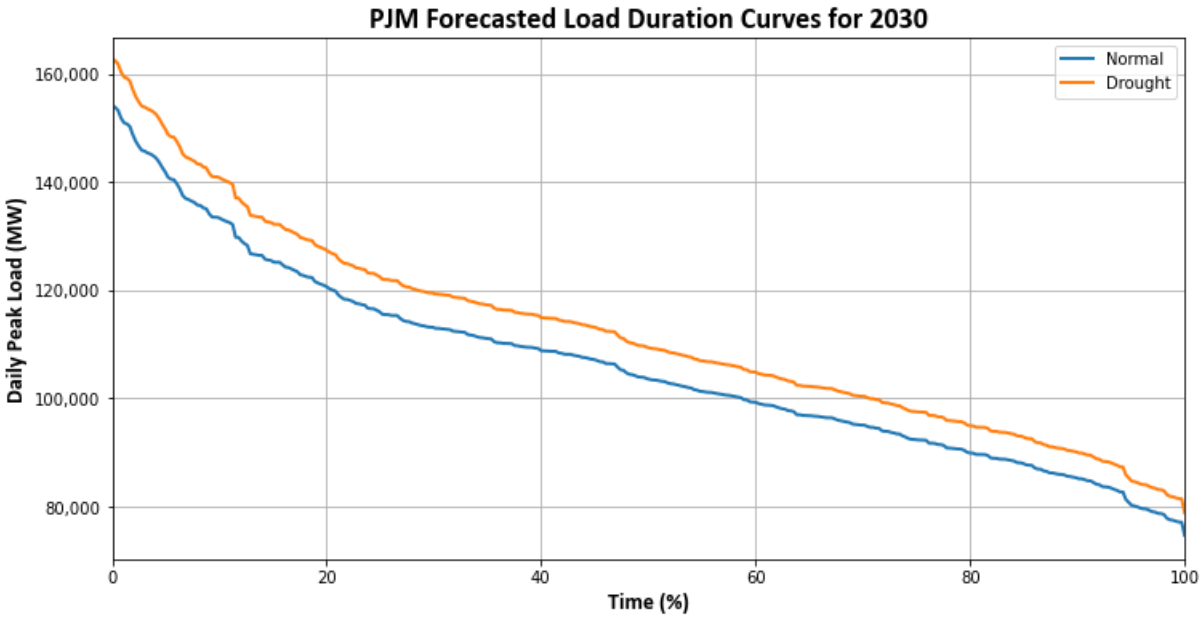

Figure 4.2: Load duration curves for the PJM region per forecasted summer 2030 values for normal and drought cases.

$$\frac{P_{hist}}{AVL_{hist}} = \frac{P_{new}}{AVL_{new}} \tag{4.6}$$

Where P_{hist} and AVL_{hist} refers to the total daily generation (MWh) and availability (%), respectively, for the *Historical Normal* scenario; and P_{new} and AVL_{new} refers to the total daily generation (MWh) and availability (%), respectively, for the drought and/or climate change scenario. These adjustments are summarized in Table 4.6.

Additionally, recall that a key feature of reliability metrics was facilitating assessments of capacity changes to the generation fleet, whether in the form of derations from extreme weather conditions, proposed capacity additions/reductions, or combinations of both. Therefore, we have the flexibility to evaluate different generation fleet compositions in terms of reliability when subjected to these drought and climate change scenarios. Specifically, we examined synthetic fleets with increased proportions of hydro and decreased proportions of coal, one and three of each, respectively, as illustrated in Figure 4.3. Per Figure 4.1, hydro accounts for less than 2% of PJM's generation fleet, whereas hydro in other regions of the U.S. and world constitutes much larger portions, so we elected to increase hydro's proportion in the generation fleet to approximately 20% [11, 19, 25]. Additionally, as discussed in Section 4.2, hydro is functionally similar to natural gas combustion turbines (in the sense of broader grid ancillary services) and thereby, in scaling up hydro's portion in the generation fleet, most of these plants will simply be treated as hydro in our reliability calculations (i.e., the FOR/AVL will reflect that of hydro instead of combustion turbine). However, there is not enough available capacity to facilitate hydro reaching the 20% mark (i.e., combustion turbines only constitute 14% of the total fleet), and since it is unlikely that this technology will be completely removed from a system, we reduced it to approximately 4%. Thus, replacing combined cycle plants was also employed, primarily due to their lion's share of the generation fleet (i.e., 32%, whereas the runner-up was coal at 16%).

On the other hand, the other synthetic fleets incorporated varying levels of coal plant retirement — 50%, 75%, and 100%, with coal attributing slightly over $35GW$ to PJM's total installed capacity (note that each greater case contains all plants in the previous case). These scenarios were selected to analyze reliability impacts if accelerations of current coal retirement plans were implemented (or the flexibility in which these plans could be

Table 4.6: Forced Outage Rates for Hydro Plants Adjusted to the Drought and Climate Change Scenarios.

Scenario	Adjustments for Hydro	
	Forced Outage Rate (%)	Availability (%)
Historical Normal	6.9725	93.0275
Historical Drought	66.0601	33.9399
Moderate Climate Change	27.5732	72.4268
Moderate Climate Change – Temperature Drought	25.6225	74.3775
Moderate Climate Change – Precipitation Drought	46.7334	53.2660
Moderate Climate Change – Drought	49.5884	20.4116
Severe Climate Change	6.90725	93.0275
Severe Climate Change – Temperature Drought	7.1118	92.8882
Severe Climate Change – Precipitation Drought	34.2167	65.7833
Severe Climate Change – Drought	37.3570	62.6430

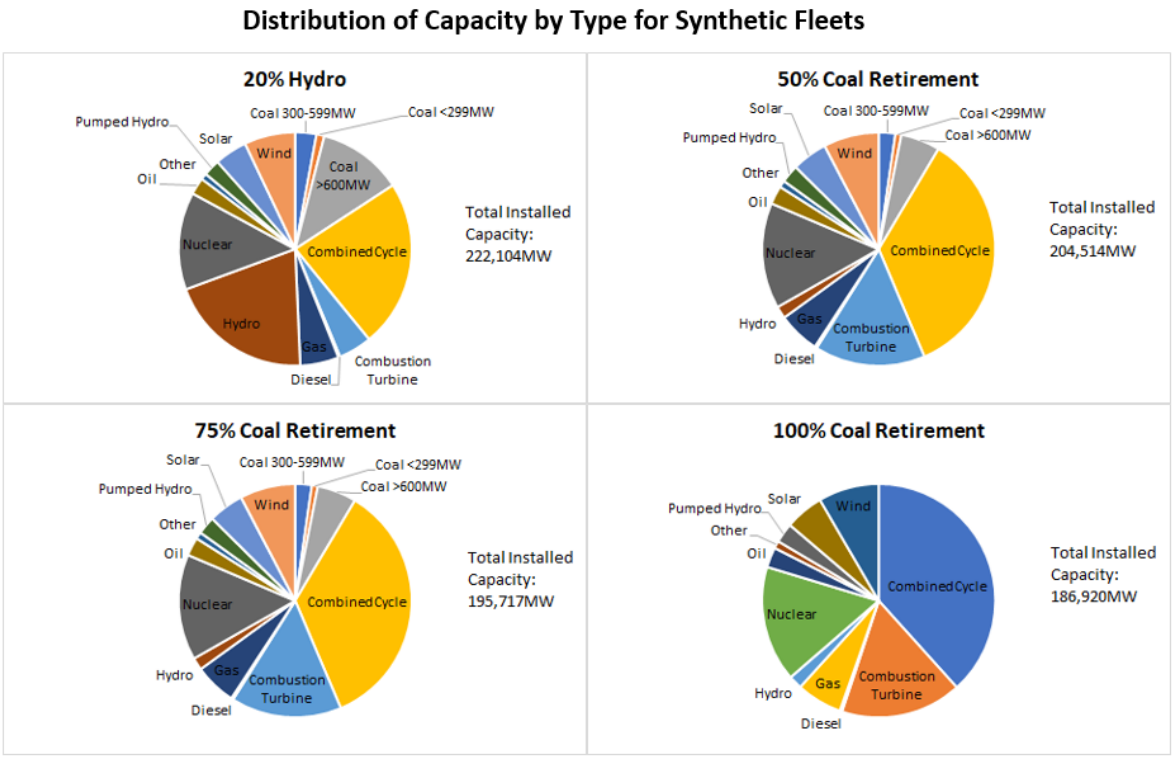

Figure 4.3: Distribution of capacity by type for each synthetic fleet.

altered). Coal was specifically chosen to reflect larger national trends, where cheaper renewables (i.e., wind and solar) and elevated operating costs (e.g., fuel acquisition, increasingly strict environmental regulation, aging infrastructure, etc.) are reducing the viability of coal power plants [101, 102]. Furthermore, consumers and regulators alike are pressuring utilities to phase out coal in favor of cleaner/greener methods of electricity generation (e.g., wind, solar, biomass, and even natural gas) [101, 102].

4.3.2 Results

Recalling the general trend of the hydrologic and generation modeling results (i.e, Sections 3.3 and 4.1.1, where the *Historical Drought* scenario was the worst case, followed by the combined and precipitation drought cases of moderate and severe climate change, respectively, and then the temperature drought and normal cases of moderate climate change, with all falling below that of the *Historical Normal* scenario. On the other hand, the *Severe Climate Change* scenario exceeded this baseline and the *Severe Climate Change – Temperature Drought* exhibited minimal deviation. Because the LOLP calculations incorporated these results (i.e., FOR/AVL for the hydro plants was based on the generation results of each scenario), a similar general trend is apparent for each fleet, albeit with slight variation likely due to the inherent variability of implementing Monte Carlo methods, as shown in Table 4.7. Here, note that zero LOLP values indicate there is sufficient available generation capacity to meet all expected loads, whereas nonzero values imply potential reliability concerns. Specifically, those above the threshold of one day per decade (i.e., a probability of 0.00027) are particularly important to understand and characterize (per U.S. regulation), which occurred in the *Historical Drought* scenario of the 20% hydro fleet and every scenario of the 75% and 100% coal retirement fleets except for the *Historical Normal* scenario in the former.

Accordingly, in the 20% hydro fleet, nonzero LOLP values only appear in the top three worst-case scenarios, illustrating a key distinction in impacts on hydropower generation between the various drought and climate change scenarios. Since all scenarios in the original fleet had zero LOLP values, these impacts are only realized when the capacity contribution of hydro is increased significantly. On the other hand, the coal retirement fleets mostly exhibited nonzero LOLP values (the few zero values only occurred in the *Historical Normal*

Table 4.7: Loss of Load Probability Results for Drought and Climate Change Scenarios Across Different PJM Generation Fleet Compositions.

Scenario	Loss of Load Probability (LOLP) Units of days/decade, with benchmark of 1 days/decade				
	Original Fleet (<2% hydro)	Synthetic Fleet (~20% hydro)	Synthetic Fleet (~50% coal retired)	Synthetic Fleet (~75% coal retired)	Synthetic Fleet (100% coal retired)
Historical Normal	0	0	0	0	1.552
Historical Drought	0	32.466	0.021	14.937	101.526
Moderate Climate Change	0	0	0.002	6.866	82.535
Moderate Climate Change – Temperature Drought	0	0	0.005	6.610	81.440
Moderate Climate Change – Precipitation Drought	0	0.204	0.005	10.226	91.665
Moderate Climate Change – Drought	0	0.650	0.014	11.102	92.761
Severe Climate Change	0	0	0	4.127	73.770
Severe Climate Change – Temperature Drought	0	0	0.005	4.200	73.770
Severe Climate Change – Precipitation Drought	0	0	8.22e-7	2.15e-3	2.34e-2
Severe Climate Change – Drought	0	0	0	2.47e-3	2.38e-2

scenario of both the 50% and 75% fleets, and the *Severe Climate Change* and *Severe Climate Change – Drought* scenarios of the 50% fleet). Additionally, both the 75% and 100% had nearly every scenario exceed the LOLP threshold, indicating that accelerating the retirement of PJM's coal fleet beyond the 50% mark can prove problematic during drought and climate change conditions (i.e., $17.5GW$ of the $35GW$ total fleet). Note that there is approximately an $8GW$ increase in load between the *Historical Normal* and drought and climate change scenarios, which in turn, has a major impact on the severity of the LOLP values (i.e., by allowing more overlap between available generation and expected load). Accordingly, if load does not increase by this amount, then the potential reliability impacts of the scenarios will not be as severe (i.e., reduced LOLP values).

Chapter 5

Conclusions

In this analysis, our goal was to characterize the potential impacts of nine drought and climate change scenarios on hydropower plants across PJM in Summer 2030 (i.e., June–September), relative to a historical baseline. Specifically, these scenarios were: *Historical Normal* (2011), *Historical Drought* (2007), *Moderate Climate Change*, *Moderate Climate Change – Drought*, *Moderate Climate Change – Temperature Drought*, *Moderate Climate Change – Precipitation Drought*, *Severe Climate Change*, *Severe Climate Change – Drought*, *Severe Climate Change – Temperature Drought*, and *Severe Climate Change – Precipitation Drought*). Recall that moderate and severe climate change was defined according to RCP 4.5 and 8.5 characteristics, respectively, and the temperature and precipitation droughts referred to increases in air temperatures by 2℃ and reductions in precipitation by 20%, respectively, with the overall drought scenarios incorporating both. Accordingly, hydropower impacts from these scenarios were quantified by modeling daily hydrologic conditions for all of the subbasins contained in PJM using HAWQS, where streamflow into and out of each was averaged together for all enclosed plants, and each plant was assumed to pass this flow as shown (i.e., no interday storage beyond what was included in the modeling process of HAWQS). Then, these resulting streamflow values were translated into total daily generation, which was utilized to characterize the severity of each scenario and the vulnerability of PJM's hydropower fleet to these conditions. Additionally, these results were translated into broader economic (using LCOE values) and reliability (using Monte Carlo-based LOLP modeling) impacts.

Across all scenarios, we found that the *Historical Drought* had the lowest total summer generation, followed by the combined drought and precipitation scenarios of the moderate and severe climate change, respectively. The base and temperature drought scenarios of moderate climate change were next on this list, whereas the temperature drought scenario of severe climate change showed little change and the base scenario actually exhibited increased generation. On a monthly basis, September generally experienced the lowest total generation, except for the *Historical Normal* scenario and the precipitation drought and combined drought scenarios of *Severe Climate Change – Drought*, where August exhibited the worst for both. Additionally, the climate change scenarios tended to reflect the *Historical Normal* conditions for the first half of summer (i.e., June and July), then match, if not, surpass the *Historical Drought* conditions during August and September. As for the 13 plants identified as most vulnerable to near complete deration (i.e., reductions in generation on the order of 99–100% relative to the *Historical Normal* scenario), most instances occurred in September of the precipitation and combined drought scenarios of moderate climate change.

With these results in mind, several key inferences can be observed — first, the compounding effects of climate change can result in more severe reductions in generation as the summer progresses, leading to a potential shift of the lowest month from August to September (relative to the *Historical Normal* scenario). While these impacts may not be as severe as the *Historical Drought* scenario for the summer overall, dramatic shifts in timing of generation still place significant stress on the power system by requiring supplementary power to compensate for the losses (assuming all lost generation here necessitates replacement). Additionally, if these climate change scenarios are expected to become more normalized occurrences, rather than occasional events like the 2007 Summer Drought, then compensation is necessary across the board for the reduced monthly and summer total generations in nearly every instance, except for the *Severe Climate Change* and *Severe Climate Change – Temperature Drought* scenarios (however, note that these still have significant reductions in September that will require compensation). Furthermore, there is also the potential for these drought and climate change conditions to have lingering effects past summer into the autumn months, especially as the historical flow regimes typically illustrated lower flows

in autumn and higher flows in winter-to-spring, which would then necessitate even greater compensation for lost generation (compared to what is normally expected).

Likewise, reductions to the generation potential of hydro also has broader consequences in terms of economics and reliability. Due to the virtually nonexistent fuel costs, any replacement from other resources will certainly reduce revenue streams, especially if these resources must be utilized in a matter requiring the operational flexibility of hydro. For instance, replacement using natural gas combustion turbines, which are the closest technology available that can mimic hydro's operational flexibility, can induce additional costs from $600 thousand upwards to $280 million across the entire summer, per the generation results of our scenarios. This would have severe impacts for both electricity producers and consumers alike. Furthermore, reductions in hydro's generation potential also decreases power system reliability by increasing the probability of insufficient available generation capacity to satisfy electricity demand. While hydro doesn't currently comprise a large enough proportion to induce significant impacts, if coal retirement plans are accelerated (beyond what is currently envisioned), these implications become much more apparent. For instance, our results showcase that a retirement of 50% does not result in LOLP values exceeding the threshold of 0.00027 (per U.S. requirements of less than one day per decade for failing to satisfy load). However, if 75% is utilized, then every scenario except the *Historical Normal* exceeds this threshold, which is then exceeded in the case where all are retired. Therefore, PJM can potentially accelerate the retirement of their coal fleet upwards of 50% without reliability concerns, but additional studies should be performed to further illustrate how much flexibility exists with regards to accelerating coal retirement, such as incorporating thermal plants into this analysis and expanding the reliability calculations employed, even possibly including transmission and distribution system constraints.

Chapter 6

Future Work

As discussed in Chapter 1 and 2, droughts and climate change can have a broad impact on the power system, far beyond just hydropower resources. For instance, other generation resources can be adversely affected, especially those reliant on water (i.e., thermal), as well as the transmission and distribution systems responsible for transmitting electricity from producer to consumer (e.g., power lines have thermal loading limits directly correlated to ambient air temperature) [1, 11, 48]. Additionally, as mentioned briefly in Section 4.3.1, electricity consumption is also impacted by weather conditions (e.g., elevated temperatures typically induce greater air conditioning usage) [1, 11, 48]. Therefore, future work can expand the impact on the generation system by including thermal (e.g., coal, combined cycle, nuclear, various renewables, etc.) and non-thermal power plants (e.g., combustion turbine, solar, wind, PSH, etc.), as well as impacts on the transmission and distribution systems by including weather-related limits. Furthermore, the effects of drought and climate change on load can also be more accurately evaluated via incorporating specific spatial and temporal parameters (e.g., relating weather conditions to load on a region-by-region scale).

Beyond including additional components of power system, some of the more integral parts of the modeling process could be further refined. For instance, a sensitivity analysis of the different variations in future drought conditions can be performed to best ascertain the most realistic case — specifically, varying levels of elevated temperature, reduced precipitation, and spatial and temporal extent can be explored. This could also include comparing multiple climate change models to capture any variability in processes. Additionally, different

reservoir operating schemes could be employed to reflect operation under stressed conditions, and hydrologic modeling could be moved to a finer level to greater characterize specific plant impacts (e.g., from the HUC-08 subbasin to HUC-10 or HUC-12, or even individual plant). However, tradeoffs between model complexity and computational efficiency must be assessed when conducting future analyses to ensure practical and useful results.

Together, these additional methods can facilitate the modeling of a system-wide unit commitment and optimal power flow study, which would result in a fine-tuned, comprehensive assessment of the range of potential effects of summer drought and climate change on the PJM region. This can of course be extended to include or encompass other regions as well, such as the Southeastern U.S. or broader Eastern U.S. power systems. Accordingly, while the results of our analysis proved insightful, there are many additional directions this body of work can be taken to further characterize these important issues.

Bibliography

[1] M. Davis and S. Clemmer, "Power Failure: How Climate Change Puts Our Electricity at Risk – and What We Can Do," *Union of Concerned Scientists*, pp. 1–16, 2014. viii, 2, 6, 7, 8, 10, 45, 71

[2] United States Department of Energy, "Types of Hydropower Plants," No Date, Accessed: 18 January 2022. [Online]. Available: https://www.energy.gov/eere/water/types-hydropower-plants viii, 11, 12, 13, 46

[3] B. Hadjerioua, K. Stewart, S. DeNeale, and *et al.*, "Pumped Storage Hydropower FAST Commissioning Technical Analysis," *ORNL/SPR-2019/1299*, pp. 1–101, 2020. viii, 13, 14, 15, 16

[4] PJM Interconnection, "Territory Served," 10 May 2021, Accessed: 18 January 2022. [Online]. Available: https://www.pjm.com/-/media/about-pjm/pjm-zones.ashx viii, 17

[5] ——, "PJM's Evolving Resource Mix and System Reliability," *Special Reports*, pp. 1–44, 2017. viii, 2, 4, 7, 15, 18, 19, 52, 57

[6] NOAA Office of Oceanic and Atmospheric Research: NIDIS Program, "DEWS Regions Drought Information," No Date, Accessed: 19 January 2022. [Online]. Available: https://www.drought.gov/dews viii, 22, 23

[7] United States Geological Survey: Water Science School, "The Fundamentals of the Water Cycle," 10 July 2019, Accessed: 27 January 2022. [Online]. Available: https://www.weather.gov/jetstream/hydro viii, 28

[8] J. G. Arnold, J. R. Kiniry, R. Srinivasan, and *et al.*, "HAWQS Calibration Process," *Version 1.0 - September 2017*, pp. 1–8, 2017. ix, 29, 30

[9] Intergovernmental Panel on Climate Change, "Climate Change 2013: The Physical Science Basis," *Working Group I Contribution to the Fifth Assessment Report of the Intergovernmental Panel on Climate Change*, pp. 1–1552, 2013. ix, 9, 22, 31, 32, 33

[10] N. Voisin, M. Kintner-Meyer, R. Skaggs, and *et al.*, "Vulnerability of the US western electric grid to hydro-climatological conditions: How bad can it get?" *Energy*, vol. 115, pp. 1–12, 2016. 1, 2, 4, 6, 7, 9, 10, 25, 33, 45

[11] C. B. Harto, Y. E. Yan, Y. K. Demissie, and *et al.*, "Analysis of Drought Impacts on Electricity Production in the Western and Texas Interconnections of the United States," *ANL/EVS/R-11/14*, pp. 1–161, 2011. 1, 2, 4, 7, 9, 10, 25, 33, 36, 45, 62, 71

[12] A. Ford, "System Dynamics and the Electric Power Industry," *System Dynamics Review*, vol. 13, no. 1, pp. 57–85, 1997. 1

[13] Y. Su, J. D. Kern, P. M. Reed, and G. W. Characklis, "Compound hydrometeorological extremes across multiple timescales drive volatility in California electricity market prices and emissions," *Applied Energy*, vol. 276, no. 115541, pp. 1–10, 2020. 1, 4, 7

[14] H. Saadat, *Power System Analysis: Third Edition*. PSA Publishing LLC, 2010. 1

[15] M. Kezunovic, I. Dobson, and Y. Dong, "Impact of Extreme Weather on Power System Blackouts and Forced Outages: New Challenges," *7th Balkan Power Conference*, pp. 1–5, 2008. 1

[16] M. T. H. van Vliet, J. Sheffield, D. Wiberg, and E. F. Wood, "Impacts of recent drought and warm years on water resources and electricity supply worldwide," *Environmental Research Letters*, vol. 11, no. 12, pp. 1–10, 2016. 1, 2, 4, 7, 9, 10, 25, 33, 45

[17] M. T. H. van Vliet, D. Wiberg, S. Leduc, and K. Riahi, "Power-generation system vulnerability and adaptation to changes in climate and water resources," *Nature Climate Change*, vol. 6, pp. 375–380, 2016. 1, 2, 4, 6, 7, 9, 10, 25, 33, 45, 46

[18] M. R. Allen-Dumas, B. KC, and C. I. Cunliff, "Extreme Weather and Climate Vulnerabilities of the Electric Grid: A Summary of Environmental Sensitivity Quantification Methods," *ORNL/TM-2019/1252*, pp. 1–27, 2019. 1, 2

[19] B. Blackshear, T. Crocker, E. Drucker, and *et al.*, "Hydropower Vulnerability and Climate Change: A Framework for Modeling the Future of Global Hydroelectric Resources," *Middlebury College Environmental Studies Senior Seminar*, pp. 1–82, 2011. 1, 10, 45, 62

[20] N. Lu, Z. T. Taylor, W. Jiang, and *et al.*, "Climate Change Impacts on Residential and Commercial Loads in the Western U.S. Grid," *PNNL-17826*, pp. 1–64, 2008. 2

[21] A. Staudt and R. Curry, "More Extreme Weather and the U.S. Energy Infrastructure," *National Wildlife Federation: Global Warming and Extreme Weather*, pp. 1–16, 2011. 2

[22] O. J. Guerra, B. Sergi, B.-M. Hodge, and *et al.*, "Electric Power Grid and Natural Gas Network Operations and Coordination," *NREL/TP-6A50-77096*, pp. 1–79, 2020. 2

[23] L. Poch, G. Conzelmann, and T. Veselka, "An Analysis of the Effects of Drought Conditions on Electric Power Generation in the Western United States," *DOE/NETL-2009/1365*, pp. 1–40, 2009. 2, 4, 7, 9, 25, 33

[24] J. Rogers, K. Averyt, S. Clemmer, and *et al.*, "Water-Smart Power: Strengthening the U.S. Electricity System in a Warming World," *Union of Concerned Scientists: Energy and Water in a Warming World Initiative*, pp. 1–58, 2013. 2, 6, 7, 10, 45

[25] A. L. Caceres, P. Jaramillo, H. S. Matthews, and *et al.*, "Hydropower under climate uncertainty: Characterizing the usable capacity of Brazilian, Colombian and Peruvian power plants under climate scenarios," *Energy for Sustainable Development*, vol. 61, pp. 217–229, 2021. 2, 7, 10, 25, 33, 45, 46, 62

[26] H. Koch and S. Vögele, "Dynamic modelling of water demand, water availability and adaptation strategies for power plants to global change," *Ecological Economics*, vol. 68, pp. 2031–2039, 2009. 2

[27] S.-C. Kao, M. Ashfaq, B. S. Naz, and *et al.*, "The Second Assessment of the Effects of Climate Change on Federal Hydropower," *ORNL/SR-2015/357*, pp. 1–308, 2016. 2, 4, 6, 7, 10, 25, 33, 36

[28] J. D. Kern, Y. Su, and J. Hill, "A retrospective study of the 2012–2016 California drought and its impacts on the power sector," *Environmental Research Letters*, vol. 15, no. 094008, pp. 1–12, 2020. 2, 4, 7

[29] B. R. Scanlon, I. Duncan, and R. C. Reedy, "Drought and the water-energy nexus in Texas," *Environmental Research Letters*, vol. 8, no. 045033, pp. 1–14, 2013. 2, 36

[30] E. Gil, Y. Morales, and T. Ochoa, "Addressing the Effects of Climate Change on Modeling Future Hydroelectric Energy Production in Chile," *Energies*, vol. 14, no. 241, pp. 1–23, 2021. 2, 4, 7, 9, 33, 36

[31] D. B. K. Milazi and L. Pratson, "The Impact of Drought on Electricity Supply in North Carolina," *Duke University Master's Project*, pp. 1–69, 2009. 2

[32] PJM Interconnection: Dispatch, "PJM Manual 12: Balancing Operations," *Revision 42*, pp. 1–114, 2021. 2

[33] PJM Interconnection: Capacity Markets and Demand Response Operations, "PJM Manual 18: PJM Capacity Market," *Revision 49*, pp. 1–274, 2021. 2

[34] PJM Interconnection, "PJM Data Miner 2," 2022, Accessed: 31 May 2022. [Online]. Available: https://dataminer2.pjm.com/list 2, 56, 57

[35] United States Department of Energy, "Hydropower Vision: A New Chapter for America's 1st Renewable Electricity Source," *ORNL/TM-2016/688*, pp. 1–407, 2016. 4, 7, 15, 16, 46

[36] D. Anghileri, M. Botter, A. Castelletti, and P. Burlando, "A Comparative Assessment of the Impact of Climate Change and Energy Policies on Alpine Hydropower," *Water Resources Research*, vol. 54, pp. 9144–9161, 2018. 4, 7, 9, 10, 25, 33, 45, 52

[37] United States Department of Energy: Office of Energy Efficiency and Renewable Energy, "Hydropower Basics," No Date, Accessed: 17 January 2022. [Online]. Available: https://www.energy.gov/eere/water/hydropower-basics 4, 10, 11, 45, 46

[38] S. Blumsack, "Basic economics of power generation, transmission and distribution," No Date, Accessed: 17 January 2022. [Online]. Available: https://www.e-education.psu.edu/eme801/node/530 4, 50, 52

[39] M. F. R. Tanteliniaina, M. H. Rahaman, and J. Zhai, "Assessment of the Future Impact of Climate Change on the Hydrology of the Mangoky River, Madagascar Using ANN and SWAT," *Water*, vol. 13, no. 1239, pp. 1–14, 2021. 6, 10, 31

[40] X. Zhang, R. Srinivasan, and F. Hao, "Predicting Hydrologic Response to Climate Change in the Luohe River Basin Using the SWAT Model," *Transactions of the ASABE*, vol. 50, no. 3, pp. 901–910, 2007. 6, 10, 25, 26, 33, 36

[41] C. A. Dieter, M. A. Maupin, R. R. Caldwell, and *et al.*, "Estimated Use of Water in the United States in 2015," *USGS Water Availability and Use Science Program: Circular 1441, Supersedes USGS Open-File Report 2017–1131*, pp. 1–76, 2017. 7

[42] Union of Concerned Scientists, "How it Works: Water for Power Plant Cooling," 15 July 2013, Accessed: 18 January 2022. [Online]. Available: https://www.ucsusa.org/resources/water-power-plant-cooling 7, 10, 45

[43] P. Ganguli, D. Kumar, , and A. R. Ganguly, "US Power Production at Risk from Water Stress in a Changing Climate," *Nature Scientific Reports*, vol. 7, no. 11983, pp. 1–13, 2017. 7, 10, 33

[44] Tara Energy, "Mechanical Energy 101: Everything You Need to Know," No Date, Accessed: 19 January 2022. [Online]. Available: https://taraenergy.com/blog/mechanical-energy-101/ 7, 11

[45] C. Auer and E. Kriegler, "What are Climate Change Scenarios?" 2020, Accessed: 18 January 2022. [Online]. Available: https://climatescenarios.org/primer/ 9, 31, 33

[46] International Union for Conservation of Nature, "WATER AND CLIMATE CHANGE: Building climate change resilience through water management and ecosystems," *Issues Brief*, 2015. 10

[47] K. N. Ogbu, E. L. Ndulue, I. E. Ahaneku, and J. I. Ubah, "Evaluation of the Impact of Climate Change on Streamflow Using SWAT Model," *ASM Science*, vol. 13, pp. 1–8, 2020. 10, 25, 26, 31, 33, 36

[48] Argonne National Laboratory, "Impacts of Long-term Drought on Power Systems in the U.S. Southwest," No Date, Accessed: 18 January 2022. [Online]. Available: https://www.energy.gov/sites/prod/files/Impacts%20of%20Long-term%20Drought%20on%20Power%20Systems%20in%20the%20US%20Southwest%20%E2%80%93%20July%202012.pdf 10, 71

[49] B. Stoll, J. Andrade, S. Cohen, and *et al.*, "Hydropower Modeling Challenges," *NREL/TP-5D00-68231*, pp. 1–29, 2017. 11, 13, 45

[50] S. DeNeale, N. Bishop, L. Buetikofer, and *et al.*, "Hydropower Geotechnical Foundations: Current Practice and Innovation Opportunities for Low-Head Applications," *ORNL/TM-2020/1553*, pp. 1–131, 2020. 11

[51] B. Afework, E. Cey, L. Goodfellow, and *et al.*, "Run-of-the-river hydroelectricity," 13 September 2018, Accessed: 18 January 2022. [Online]. Available: https://energyeducation.ca/encyclopedia/Run-of-the-river_hydroelectricity 11, 13

[52] United States Energy Information Administration, "Electricity explained: Electricity generation, capacity, and sales in the United States," 18 March 2021, Accessed: 18 January 2022. [Online]. Available: https://www.eia.gov/energyexplained/electricity/electricity-in-the-us-generation-capacity-and-sales.php 15

[53] K. S. Ratnam, K. Palanisamy, and G. Yang, "Future low-inertia power systems: Requirements, issues, and solutions - A review," *Renewable and Sustainable Energy Reviews*, vol. 124, no. 109773, pp. 1–24, 2020. 15

[54] J. R. Gracia, P. W. O'Connor, , L. C. Markel, and *et al.*, "Hydropower Plants as Black-Start Resources," *ORNL/SPR-2018/1077*, pp. 1–75, 2019. 15, 16

[55] R. Uría-Martínez, M. M. Johnson, and R. Shan, "U.S. Hydropower Market Report: January 2021," *DOE/EE-2088*, pp. 1–158, 2021. 15, 16, 18

[56] Sustainable FERC Project, "Understanding Energy: PJM Explained," *Policies for a Clean Electric Grid*, pp. 1–5, No Date. 16, 18

[57] PJM Interconnection, "PJM History," No Date, Accessed: 18 January 2022. [Online]. Available: https://www.pjm.com/about-pjm/who-we-are/pjm-history 16, 18

[58] ——, "Who We Are," No Date, Accessed: 18 January 2022. [Online]. Available: https://www.pjm.com/about-pjm/who-we-are 16

[59] Pennsylvania Public Utility Commission, "Summer 2021: PJM Reliability Assessment," May 2021, Accessed: 20 January 2022. [Online]. Available: https://www.puc.pa.gov/media/1551/summer_reliability_2021-pjm.pdf 16

[60] Monitoring Analytics, LLC, "State of the Market Report for PJM," *Volume I and II*, pp. 1–776, 2020. 18

[61] M. M. Johnson, "Existing Hydropower Assets (EHA) Capacity Plant Database, 2005–2019," *HydroSource*, 2021. 20, 46

[62] Energy Information Administration, "Electricity: Form EIA-860 detailed data with previous form data (EIA-860A/860B)," *Data*, 2021. 20, 45, 46, 56, 57

[63] Federal Energy Regulatory Commission, "Hydropower," No Date, Accessed: 20 January 2022. [Online]. Available: https://www.ferc.gov/industries-data/hydropower 20

[64] National Oceanic and Atmospheric Administration: Office of Oceanic and Atmospheric Research, "NIDIS Program," No Date, Accessed: 19 January 2022. [Online]. Available: https://www.drought.gov/ 22

[65] National Oceanic and Atmospheric Administration: Office of Oceanic and Atmospheric Research – NIDIS Program, "DROUGHT EARLY WARNING SYSTEM: Northeast," No Date, Accessed: 19 January 2022. [Online]. Available: https://www.drought.gov/dews/northeast 22

[66] ——, "DROUGHT EARLY WARNING SYSTEM: Southeast," No Date, Accessed: 19 January 2022. [Online]. Available: https://www.drought.gov/dews/southeast 22

[67] ——, "DROUGHT EARLY WARNING SYSTEM: Midwest," No Date, Accessed: 19 January 2022. [Online]. Available: https://www.drought.gov/dews/midwest 22

[68] O. Tamm, A. Luhamaa, and T. Tamm, "Modeling future changes in the North-Estonian hydropower production by using SWAT," *Hydrology Research*, vol. 47, no. 4, pp. 1–12, 2016. 25

[69] R. Horan, R. Gowri, P. S. Wable, and *et al.*, "A Comparative Assessment of Hydrological Models in the Upper Cauvery Catchment," *Water*, vol. 13, no. 151, pp. 1–25, 2021. 25, 26, 33

[70] University of Washington, "Variable Infiltration Capacity (VIC) Model," January 2015, Accessed: 24 January 2022. [Online]. Available: http://www.appsolutelydigital.com/ModelPrimer/chapter5_section9.html#:~:text=The%20VIC%20model%2C%20first%20developed,full%20water%20and%20energy%20balances.&text=The%20model%20can%20be%20used,management%2C%20and%20climate%20change%20studies 25, 26

[71] S. L. Neitsch, J. G. Arnold, J. R. Kiniry, and J. R. Williams, "Soil and Water Assessment Tool: Theoretical Documentation, Version 2009," *TR-406*, pp. 1–647, 2011. 25, 26, 27, 33

[72] J. G. Arnold, J. R. Kiniry, R. Srinivasan, and *et al.*, "Soil and Water Assessment Tool: Input/Output Documentation, Version 2012," *TR-439*, pp. 1–650, 2012. 26, 27, 29

[73] C. Fant, R. Srinivasan, B. Boehlert, and *et al.*, "Climate Change Impacts on US Water Quality Using Two Models: HAWQS and US Basins," *Water*, vol. 9, no. 119, pp. 1–21, 2017. 26

[74] Texas A&M AgriLife Research Spatial Sciences Laboratory, "HAWQS System and Data to model the lower 48 conterminous U.S using the SWAT model," *Texas Data Repository Dataverse, Version 1*, 2020. 26, 29, 31

[75] Texas A&M: AgriLife Research Spatial Sciences Laboratory, "HAWQS User Guide," *Version 1.1*, pp. 1–88, 2019. 26, 27

[76] M. E. Muche, S. Sinnathamby, R. Parmar, and *et al.*, "Comparison and Evaluation of Gridded Precipitation Datasets in a Kansas Agricultural Watershed Using SWAT," *Journal of the American Water Resources Association*, vol. 56, no. 3, pp. 486–506, 2020. 29

[77] M. S. Buban, T. R. Lee, and C. B. Baker, "A Comparison of the U.S. Climate Reference Network Precipitation Data to the Parameter-Elevation Regressions on Independent Slopes Model (PRISM)," *Journal of Hydrometeorology*, vol. 21, no. 10, pp. 2391–2400, 2020. 29

[78] R. Bhandari, A. Kalra, and S. Kumar, "Analyzing the Effect of CMIP5 Climate Projections on Streamflow Within the Pajaro River Basin," *Open Water*, vol. 6, no. 1, pp. 1–25, 2020. 31

[79] J. Caesar, E. Palin, S. Liddicoat, and *et al.*, "Response of the HadGEM2 Earth System Model to Future Greenhouse Gas Emissions Pathways to the Year 2300*," *Journal of Climate*, vol. 26, no. 20, pp. 3275–3284, 2013. 31

[80] SWAT User Group, "How to set up warm-up period in SWAT," 20 July 2016, Accessed: 29 January 2022. [Online]. Available: https://groups.google.com/g/arcswat/c/c19Li5ATNvY 36

[81] ——, "Re: warming up SWAT," 13 March 2009, Accessed: 29 January 2022. [Online]. Available: https://groups.google.com/g/swatuser/c/UDV9rEd3irQ 36

[82] D. dos Reis Pereira, A. Q. de Almeida, M. A. Martinez, and D. R. Q. Rosa, "Impacts of deforestation on water balance components of a watershed on the Brazilian East Coast," *Soil Use and Management*, vol. 38, no. 4, pp. 1350–1358, 2014. 36

[83] A. G. Mengistua, L. D. van Rensburga, and Y. E. Woyessab, "Techniques for calibration and validation of SWAT model in data scarce arid and semi-arid catchments in South Africa," *Journal of Hydrology: Regional Studies*, vol. 25, no. 100621, pp. 1–18, 2019. 36

[84] F. K. Musyoka, P. Strauss, G. Zhao, and *et al.*, "Multi-Step Calibration Approach for SWAT Model Using Soil Moisture and Crop Yields in a Small Agricultural Catchment," *Water*, vol. 13, no. 16, pp. 2238–2264, 2021. 36

[85] United States Geological Survey, "USGS Water Data for the Nation," 2022, Accessed: 23 May 2022. [Online]. Available: https://waterdata.usgs.gov/nwis 38

[86] P. March and P. Jacobson, "Industry Experience with Power Generation Options for Environmental Flows," *EPRI Technical Report 3002003711*, pp. 1–56, 2014. 45

[87] World Bank Group, "Environmental Flows for Hydropower Projects: Guidance for the Private Sector in Emerging Markets," *Good Practice Handbook*, pp. 1–154, 2018. 45

[88] United States Army Corps of Engineers, "National Inventory of Dams: More than 90,000 nationwide," 2020, Accessed: 2 February 2022. [Online]. Available: https://nid.sec.usace.army.mil/#/ 47

[89] Math is Fun, "Percentage Change," 2020, Accessed: 25 May 2022. [Online]. Available: https://www.mathsisfun.com/numbers/percentage-change.html 47

[90] U. S. E. I. Administration, "Levelized Costs of New Generation Resources in the Annual Energy Outlook 2022," *Annual Energy Outlook 2022*, pp. 1–26, 2022. 52

[91] A. M. Al-Shaalan, "Reliability and Maintenance - An Overview of Cases: Chapter 8 – Reliability Evaluation of Power Systems," *IntechOpen*, pp. 1–25, 2019. 54, 55, 57, 60

[92] R. Billinton and R. M. Allan, "Reliability Evaluation of Power Systems," *Plenum Press*, pp. 1–446, 1984. 54, 55, 57, 60

[93] H. F. Boroujeni, M. Eghtedari, M. Abdollahi, and *et al.*, "Calculation of generation system reliability index: Loss of Load Probability," *Life Sciences*, vol. 9, no. 4, pp. 4903–4908, 2012. 55, 57, 60

[94] J. Whittwer, "A Practical Guide to Monte Carlo Simulation," 2004, Accessed: 31 May 2022. [Online]. Available: https://www.vertex42.com/ExcelArticles/mc/MonteCarloSimulation.html 55

[95] P. Denholm and J. Katz, "USING WIND AND SOLAR TO RELIABLY MEET ELECTRICITY DEMAND," *NREL/FS-6A20-63038*, pp. 1–2, 2015. 56, 57

[96] PJM Interconnection: Resource Adequacy Planning Department, "PJM Load Forecast Report – January 2010," , pp. 1–80, 2010. 57, 60

[97] ——, "PJM Load Forecast Report – January 2015," , pp. 1–106, 2015. 57, 60

[98] ——, "PJM Load Forecast Report – January 2020," , pp. 1–89, 2020. 57, 60

[99] ——, "PJM Load Forecast Report – January 2021," , pp. 1–85, 2021. 57, 60

[100] ——, "PJM Load Forecast Report – January 2022," , pp. 1–88, 2022. 57, 60

[101] E. Howland, "Coal plant owners seek to shut 3.2 GW in PJM in face of economic, regulatory and market pressures," 2022, Accessed: 3 June 2022. [Online]. Available: https://www.utilitydive.com/news/coal-plant-owners-seek-to-retire-power-in-pjm/620781/ 65

[102] D. Sweeney and A. Duquiatan, "Outlook 2022: PJM to see 9.5-GW net gain despite surge in coal plant retirements,"

2022, Accessed: 3 June 2022. [Online]. Available: https://www.spglobal.com/marketintelligence/en/news-insights/latest-news-headlines/outlook-2022-pjm-to-see-9-5-gw-net-gain-despite-surge-in-coal-plant-retirements-69208592 65

Appendix

A Additional Details Regarding PJM's Hydropower Fleet

Additional details regarding PJM's hydropower fleet are illustrated by Tables A1 and A2, sourced from the EIA, ORNL HydroSource, and NID databases. Both tables contain general identifying information for each plant (i.e., name and EIA code). The former is dedicated to spatial data (e.g., county, state, latitude, longitude, and water source) and the latter encompasses information important to performing the quantitative analyses presented in Sections 3 and 4, such as operational mode (i.e., HYC or PSH); installed capacity (MW); NID dam name and associated dam height (m, noting that this was converted from the original ft units of the NID Database), where both of these values are listed as N/A for PSH plants because (1) they were excluded from this analysis and (2) typically two dams are required for characterization; and HUC08 region. Note that there is some variability in plant name between different sources — the ORNL HydroSource database lists both the named used in the EIA database and the name most commonly associated with the plant, the former of which is used in this dataset.

Table A1: PJM Hydropower Fleet (as of 2030) – Locational Data

EIA Code	Name	County	State	Latitude	Longitude	Water Source
903	Rockton	Winnebago	IL	42.4511	-89.0756	Rock River
986	Elkhart	Elkhart	IN	41.6928	-85.965	St Joseph River
989	Twin Branch	St Joseph	IN	41.665	-86.1322	St Joseph River
1359	Mother Ann Lee	Mercer	KY	37.8297	-84.7247	Kentucky River
1567	Deep Creek	Garrett	MD	39.523	-79.413	Deep Creek Lake
1574	Conowingo	Harford	MD	39.6572	-76.1752	Susquehanna River
1753	Berrien Springs	Berrien	MI	41.9439	-86.3289	St Joseph River
1754	Buchanan (MI)	Berrien	MI	41.839566	-86.35105	St Joseph River
1760	Constantine	St Joseph	MI	41.8436	-85.6694	St Joseph River
1761	Mottville	St Joseph	MI	41.8056	-85.7505	St Joseph River
1856	Hydro Plant	St Joseph	MI	41.9711	-85.5381	St Joseph River
2756	Gaston	Halifax	NC	36.499147	-77.811543	Roanoke River
2758	Roanoke Rapids	Halifax	NC	36.4789	-77.6722	Roanoke River
3117	York Haven	York	PA	40.113625	-76.71195	Willis Run
3124	Piney	Clarion	PA	41.192088	-79.433501	Clarion River
3145	Holtwood	Lancaster	PA	39.827198	-76.331772	Octoraro Crek
3153	Wallenpaupack	Wayne	PA	41.467858	-75.130895	Lackawaxen River
3164	Muddy Run	Lancaster	PA	39.8076	-76.2993	Susquehanna River
3175	Safe Harbor	Lancaster	PA	39.9244	-76.39	Susquehanna River
3772	Buck Hydro	Carroll	VA	36.808229	-80.938714	New River
3773	Byllesby 2	Carroll	VA	36.7858	-80.9333	New River
3774	Claytor	Pulaski	VA	37.075	-80.5847	New River
3777	Leesville	Pittsylvania	VA	37.0933	-79.4025	Roanoke River
3778	Niagara	Roanoke	VA	37.2544	-79.8756	Roanoke River
3779	Reusens	Campbell	VA	37.4639	-79.1856	James River
3780	Smith Mountain	Pittsylvania	VA	37.0413	-79.5356	Roanoke River
3789	Luray Hydro Station	Page	VA	38.676667	-78.498888	Shenandoah River
3790	Newport Hydro Station	Page	VA	38.571389	-78.593611	Shenandoah River
3798	Cushaw	Amherst	VA	37.592887	-79.380823	James River
3821	Snowden	Bedford	VA	37.5736	-79.3715	James River

Table A1 Continued

EIA Code	Name	County	State	Latitude	Longitude	Water Source
3825	Pinnacles	Patrick	VA	36.666866	-80.447897	Dan River
3826	Martinsville	Henry	VA	36.664145	-79.883588	Smith River
3827	Radford	Pulaski	VA	37.078366	-80.572726	Little River
3833	John H Kerr	Mecklenburg	VA	36.59943	-78.3005	Reservoir
3834	Philpott Lake	Henry	VA	36.7803	-80.0281	Reservoir
4258	Greenup Hydro	Scioto	OH	38.6472	-82.8594	Ohio River
6006	Racine	Meigs	OH	38.9153	-81.9081	Ohio River
6167	Bath County	Bath	VA	38.20889	-79.8	Back Creek
6168	North Anna	Louisa	VA	38.06	-77.7897	North Anna River
6171	Laurel Dam	Laurel	KY	36.9614	-84.27	Laurel River
6522	Yards Creek	Warren	NJ	41.0006	-75.0314	Creek Reservoirs
6543	Dam No. 4 Hydro Station	Jefferson	WV	39.493056	-77.826944	Potomac River
6544	Dam No. 5 Hydro Station	Berkeley	WV	39.605	-77.923055	Potomac River
6546	Millville Hydro Station	Jefferson	WV	39.273056	-77.784444	Shenandoah River
6560	London	Kanawha	WV	38.1944	-81.3706	Kanawha River
6561	Marmet	Kanawha	WV	38.2526	-81.5695	Kanawha River
6562	Winfield	Putnam	WV	38.5274	-81.91392	Kanawha River
6636	Lake Lynn Hydro Station	Fayette	PA	39.720278	-79.856111	Gressy Run
7128	William F Matson Generating Station	Huntingdon	PA	40.432915	-78.002887	Raystown Branch Juniata River
7279	O'Shaughnessy Hydro	Delaware	OH	40.153328	-83.126719	O'Shaughnessy Reservoir
7594	Belleville Dam	Wood	WV	39.1192	-81.7375	Ohio River
7657	Auglaize Hydro	Defiance	OH	41.237206	-84.399756	Auglaize River
7807	Hamilton Hydro	Butler	OH	39.4128	-84.5558	Great Miami River
8225	Seneca Generation LLC	Warren	PA	41.8389	-79.0056	Kinzua Reservoir
10152	Warrior Ridge Hydro	Huntingdon	PA	40.540042	-78.034628	Juniata River
10155	Brasfield	Chesterfield	VA	37.220833	-77.524504	Appomattox River
10285	Townsend Hydro	Beaver	PA	40.733545	-80.314795	Beaver River
10546	Beaver Valley Patterson Dam	Beaver	PA	40.744105	-80.317839	Beaver River
10656	French Paper Hydro	Berrien	MI	41.8203	-86.2592	St Joseph River
10798	Fries Hydroelectric Project	Grayson	VA	36.715103	-80.985621	New River
10903	Lockport Powerhouse	Will	IL	41.5697	-88.0789	Chicago Sanitary Ship Canal

Table A1 Continued

EIA Code	Name	County	State	Latitude	Longitude	Water Source
50010	Glen Ferris Hydro	Fayette	WV	38.1483	-81.2147	Kanawaha River
50011	Hawks Nest Hydro	Fayette	WV	38.1478	-81.1753	New River
50036	New Martinsville Hannibal Hydro	Wetzel	WV	39.6672	-80.8642	Ohio River
50175	Emporia	Greensville	VA	36.696	-77.56	Meherrin River
50178	Halifax	Halifax	VA	36.7817	-78.9236	Banister River
50311	Passaic Valley Water Commission	Passaic	NJ	40.883345	-74.22999	Passaic River
50479	Georgia-Pacific Big Island	Bedford	VA	37.534	-79.357	James River
50893	Allegheny No. 5 Hydro Station	Armstrong	PA	40.682875	-79.665298	Allegheny River
50894	Allegheny No 6 Hydro Station	Armstrong	PA	40.716389	-79.577222	Allegheny River
50897	Allegheny Hydro No 8	Armstrong	PA	40.896596	-79.478982	Allegheny River
50898	Allegheny Hydro No 9	Armstrong	PA	40.955961	-79.550681	Allegheny River
52036	Yough Hydro Power	Somerset	PA	39.801637	-79.368214	Youghiogheny River Lake
52068	Great Falls Hydro Project	Passaic	NJ	40.915319	-74.180986	Passaic River
52173	Conemaugh Hydro Plant	Westmoreland	PA	40.46439	-79.365703	Conemaugh River
54525	Kankakee Hydro Facility	Kankakee	IL	41.1128	-87.8681	Kankakee River
54655	Schoolfield Dam	Pittsylvania	VA	36.576778	-79.432503	Dan River
54969	Dixon Hydroelectric Dam	Lee	IL	41.845306	-89.481286	Rock River
56313	Coleman Falls	Bedford	VA	37.5035	-79.3006	James River
56314	Holcomb Rock	Lynchburg City	VA	37.5035	-79.3006	James River
56333	Gauley River Power Partners	Nicholas	WV	38.21921	-80.89061	Gauley River
56872	Meldahl Hydroelectric Project	Bracken	KY	38.791431	-84.172982	Ohio River
57401	Willow Island Hydroelectric Plant	Pleasants	WV	39.35776	-81.31795	Ohio River
58685	Mahoning Creek Hydroelectric Project	Armstrong	PA	40.921111	-79.281667	Mahoning Creek
58827	Flannagan Hydroelectric Project	Dickenson	VA	37.233333	-82.348611	Flannagan Dam
59091	Braddock Lock and Dam	Allegheny	PA	40.388889	-79.858889	Monogahela River
62384	Point Marion L&D Hydroelectric Project	Fayette	PA	39.726855	-79.910126	Monongahela River
62385	Maxwell L&D Hydroelectric Project	Fayette	PA	40.002401	-79.958827	Monongahela River
62386	Opekiska L&D Hydroelectric Project	Monongalia	WV	39.564917	-80.051137	Monongahela River
62387	Morgantown L&D Hydroelectric Project	Monongalia	WV	39.619589	-79.968111	Monongahela River
62388	Grays Landing L&D Hydroelectric Project	Greene	PA	39.823738	-79.923022	Monongahela River
62390	KY No. 11 L&D Hydroelectric Project	Estill	KY	37.784171	-84.102977	Kentucky River

Table A1 Continued

EIA Code	Name	County	State	Latitude	Longitude	Water Source
62400	Montgomery L&D Hydroelectric Project	Beaver	PA	40.652478	-80.386872	Ohio River
62401	Allegheny L&D2 Hydroelectric Project	Allegheny	PA	40.89444	-79.913611	Allegheny River
62403	Beverly L&D Hydroelectric Project	Washington	OH	39.555073	-81.646517	Muskingum River
62404	Monongahela L&D4 Hydroelectric Project	Washington	PA	40.145943	-79.900948	Monongahela River
62426	Rokeby L&D Hydroelectric Project	Morgan	OH	39.731999	-81.9093	Muskingum River
62427	Philo L&D Hydroelectric Project	Muskingum	OH	39.870343	-81.90977	Muskingum River
62428	Malta L&D Hydroelectric Project	Morgan	OH	39.643477	-81.850517	Muskingum River
62429	Lowell L&D Hydroelectric Project	Washington	OH	39.528315	-81.517046	Muskingum River
62433	Emsworth L&D Hydroelectric Project	Allegheny	PA	40.50305	-80.08944	Ohio River
62434	Emsworth BC Hydroelectric Project	Allegheny	PA	40.50083	-80.103055	Ohio River
62435	Devola L&D Hydroelectric Project	Washington	OH	39.469041	-81.491982	Muskingum River
62747	Ravenna Hydroelectric Project	Estill	KY	37.677484	-83.948553	Kentucky River
62748	Evelyn Hydroelectric Project	Lee	KY	37.601982	-83.832973	Kentucky River
62749	Heidelberg Hydroelectric Project	Lee	KY	37.552399	-83.770011	Kentucky River
62918	Notre Dame Hydro	St Joseph	IN	41.676	-86.2453	Saint Joseph River
64171	Tygart Hydropower	Taylor	WV	39.279354	-80.00891	Tygart Dam

Table A2: PJM Hydropower Fleet (as of 2030) – Modeling Data

EIA Code	Name	Type	Capacity (MW)	NID Dam Name	Dam Height (m)	HUC08
903	Rockton	HYC	1.1	Rockton	2.13	07090003
986	Elkhart	HYC	3.4	Elkhart	7.47	04050001
989	Twin Branch	HYC	4.8	Twin Branch	12.50	04050001
1359	Mother Ann Lee	HYC	2.1	Kentucky River Lock & Dam 7	7.32	05100205
1567	Deep Creek	HYC	20.0	Deep Creek Dam	24.99	05020006
1574	Conowingo	HYC	530.8	Conowingo (MD)	31.70	02050306
1753	Berrien Springs	HYC	7.2	Berrien Springs Dam	10.97	04050001
1754	Buchanan (MI)	HYC	4.4	Buchanan	7.01	04050001
1760	Constantine	HYC	1.2	Constantine	9.14	04050001
1761	Mottville	HYC	1.6	Mottville	7.01	04050001
1856	Hydro Plant	HYC	2.2	Sturgis	7.62	04050001
2756	Gaston	HYC	177.6	Gaston	30.18	03010106
2758	Roanoke Rapids	HYC	100.0	Roanoke Rapids	21.95	03010107
3117	York Haven	HYC	19.6	York Haven Headrace	6.10	02050305
3124	Piney	HYC	30.0	Piney	39.32	05010005
3145	Holtwood	HYC	247.3	Holtwood	16.76	02050306
3153	Wallenpaupack	HYC	40.0	Wilsonville	20.73	02040103
3164	Muddy Run	PSH	1072.0	N/A	N/A	02050306
3175	Safe Harbor	HYC	417.5	Safe Harbor	22.86	02050306
3772	Buck Hydro	HYC	8.4	Buck	13.72	05050001
3773	Byllesby 2	HYC	21.6	Byllesby	19.20	05050001
3774	Claytor	HYC	74.8	Claytor	42.37	05050001
3777	Leesville	HYC	40.0	Leesville	27.43	03010101
3778	Niagara	HYC	3.6	Niagara	18.29	03010101
3779	Reusens	HYC	12.5	Reusens	12.19	02080203
3780	Smith Mountain	PSH	547.5	N/A	N/A	03010101
3789	Luray Hydro Station	HYC	1.6	Luray	6.68	02070005
3790	Newport Hydro Station	HYC	1.4	Newport	8.53	02070005
3798	Cushaw	HYC	7.5	Cushaw	7.92	02080203
3821	Snowden	HYC	5.0	Bedford	5.97	02080203

Table A2 Continued

EIA Code	Name	Type	Capacity (MW)	NID Dam Name	Dam Height (m)	HUC-08
3825	Pinnacles	HYC	11.1	Townes	40.54	03010103
3826	Martinsville	HYC	1.3	Smith River Dam	11.58	03010103
3827	Radford	HYC	1.0	Radford	15.85	05050001
3833	John H Kerr	HYC	296.8	John H Kerr Dam	43.89	03010102
3834	Philpott Lake	HYC	14.0	Philpott Dam	67.06	03010103
4258	Greenup Hydro	HYC	70.2	Greenup L&D	23.77	05090103
6006	Racine	HYC	47.4	Racine L&D	30.48	05030202
6167	Bath County	PSH	2862.0	N/A	N/A	02080201
6168	North Anna	HYC	1.0	North Anna Cat I Service Water Dike	11.28	02080106
6171	Laurel Dam	HYC	70.0	Laurel Dam	85.95	05130101
6522	Yards Creek	PSH	453.0	N/A	N/A	02040105
6543	Dam No. 4 Hydro Station	HYC	1.9	Potomac River Dam #4	6.10	02070004
6544	Dam No. 5 Hydro Station	HYC	1.0	Potomac Dam No. 5	6.10	02070004
6546	Millville Hydro Station	HYC	2.8	Millville Dam	3.96	02070007
6560	London	HYC	14.4	London L&D	31.39	05050006
6561	Marmet	HYC	14.4	Marmet L&D	30.78	05050006
6562	Winfield	HYC	24.5	Winfield L&D	33.53	05050008
6636	Lake Lynn Hydro Station	HYC	51.2	Lake Lynn Dam (WV)	38.10	05020004
7128	William F Matson Generating Station	HYC	21.7	Raystown Dam - Hesston Dike	68.58	02050303
7279	O'Shaughnessy Hydro	HYC	5.2	O'Shaughnessy	23.93	05060001
7594	Belleville Dam	HYC	42.0	Belleville L&D	39.62	05030202
7657	Auglaize Hydro	HYC	3.6	Auglaize Hydro	7.62	04100007
7807	Hamilton Hydro	HYC	2.2	Hamilton Electric Project Dams	7.32	05080002
8225	Seneca Generation LLC	PSH	469.0	N/A	N/A	05010001
10152	Warrior Ridge Hydro	HYC	2.8	Warrior Ridge	8.23	02050302
10155	Brasfield	HYC	2.9	Brasfield (Appomattox)	22.25	02080207
10285	Townsend Hydro	HYC	5.2	Townsend	3.96	05030104
10546	Beaver Valley Patterson Dam	HYC	1.2	Upper Beaver Falls	8.23	05030104
10656	French Paper Hydro	HYC	1.3	French Paper Company Dam	6.71	04050001
10798	Fries Hydroelectric Project	HYC	5.4	Fries	12.50	05050001
10903	Lockport Powerhouse	HYC	16.0	Lockport Lock	19.81	07120004

Table A2 Continued

EIA Code	Name	Type	Capacity (MW)	NID Dam Name	Dam Height (m)	HUC-08
50010	Glen Ferris Hydro	HYC	6.2	Gauley Junction Dam	31.09	05050006
50011	Hawks Nest Hydro	HYC	102.0	Gauley Junction Dam	31.09	05050004
50036	New Martinsville Hannibal Hydro	HYC	37.4	Hannibal Locks and Dam	15.54	05030201
50175	Emporia	HYC	2.5	Emporia	13.11	03010204
50178	Halifax	HYC	1.6	Halifax	11.28	03010105
50311	Passaic Valley Water Commission	HYC	2.4	Beatties Mill Dam	3.66	02030103
50479	Georgia-Pacific Big Island	HYC	0.4	Big Island	5.49	02080203
50893	Allegheny No. 5 Hydro Station	HYC	9.2	Allegheny Lock and Dam 05	4.88	05010006
50894	Allegheny No 6 Hydro Station	HYC	9.2	Allegheny Lock and Dam 06	6.40	05010006
50897	Allegheny Hydro No 8	HYC	13.6	Allegheny Lock and Dam 08	18.29	05010006
50898	Allegheny Hydro No 9	HYC	17.8	Allegheny Lock and Dam 09	16.76	05010006
52036	Yough Hydro Power	HYC	12.2	Youghiogheny Dam	56.08	05020006
52068	Great Falls Hydro Project	HYC	12.3	Great Falls	3.66	02030103
52173	Conemaugh Hydro Plant	HYC	15.0	Conemaugh Dam	43.89	05010007
54525	Kankakee Hydro Facility	HYC	1.2	Kankakee	4.57	07120001
54655	Schoolfield Dam	HYC	4.5	Schoolfield Dam	7.62	03010103
54969	Dixon Hydroelectric Dam	HYC	3.0	Dixon	5.18	07090005
56313	Coleman Falls	HYC	1.5	Coleman Falls	6.10	02080203
56314	Holcomb Rock	HYC	1.8	Holcomb Rock	11.89	02080203
56333	Gauley River Power Partners	HYC	80.0	Summersville Dam	118.87	05050005
56872	Meldahl Hydroelectric Project	HYC	105.0	Cpt. Anthony Meldahl L&D	42.06	05090201
57401	Willow Island Hydroelectric Plant	HYC	44.0	Willow Island L&D	33.83	05030201
58685	Mahoning Creek Hydroelectric Project	HYC	6.0	Mahoning Creek Dam	49.38	05010006
62918	Notre Dame Hydro	HYC	2.5	South Bend	3.66	05070202
62390	KY No. 11 L&D Hydroelectric Project	HYC	2.5	Kentucky River Lock and Dam No. 11	10.67	05020005
62747	Ravenna Hydroelectric Project	HYC	2.5	Kentucky River Lock & Dam 12	9.45	05020003
62748	Evelyn Hydroelectric Project	HYC	3.0	Kentucky River Lock & Dam 13	13.11	05020005
62749	Heidelberg Hydroelectric Project	HYC	2.5	Kentucky River Lock & Dam 14	9.75	05020003
62403	Beverly L&D Hydroelectric Project	HYC	3.0	Muskingum River Lock and Dam No. 4	5.18	05020003
62426	Rokeby L&D Hydroelectric Project	HYC	4.0	Muskingum River Lock and Dam No. 8	6.10	05020005
62427	Philo L&D Hydroelectric Project	HYC	3.0	Muskingum River Lock and Dam No. 9	5.52	05100204

Table A2 Continued

EIA Code	Name	Type	Capacity (MW)	NID Dam Name	Dam Height (m)	HUC-08
62428	Malta L&D Hydroelectric Project	HYC	4.0	Muskingum River Lock and Dam No. 7	4.63	05030101
62429	Lowell L&D Hydroelectric Project	HYC	5.0	Muskingum River Lock and Dam No. 3	5.36	05030105
62435	Devola L&D Hydroelectric Project	HYC	4.0	Muskingum River Lock and Dam No. 2	5.33	05040004
59091	Braddock Lock and Dam	HYC	5.3	Braddock Locks and Dam	10.06	05020005
62384	Point Marion L&D Hydroelectric Project	HYC	5.0	Point Marion Lock and Dam	15.85	05040004
62385	Maxwell L&D Hydroelectric Project	HYC	12.0	Maxwell Locks and Dam	17.07	05040004
62388	Grays Landing L&D Hydroelectric Project	HYC	12.0	Grays Landing Lock and Dam	10.06	05040004
62400	Montgomery L&D Hydroelectric Project	HYC	20.4	Montgomery Locks and Dam	18.90	05040004
62401	Allegheny L&D2 Hydroelectric Project	HYC	9.0	Allegheny Lock and Dam 02	15.85	05030101
62404	Monongahela L&D4 Hydroelectric Project	HYC	12.0	Monongahela Locks and Dam 03	4.88	05030101
62433	Emsworth L&D Hydroelectric Project	HYC	20.4	Emsworth Locks and Dams	7.62	05040004
62434	Emsworth BC Hydroelectric Project	HYC	12.0	Emsworth Locks and Dams	7.62	05100204
58827	Flannagan Hydroelectric Project	HYC	1.6	John W Flannagan Dam	76.20	05100204
62386	Opekiska L&D Hydroelectric Project	HYC	6.0	Opekiska Lock and Dam	15.85	05100204
62387	Morgantown L&D Hydroelectric Project	HYC	5.0	Morgantown Lock and Dam	10.97	04050001
64171	Tygart Hydropower	HYC	30.0	Tygart Dam	71.32	05020001

Vita

William Tingen was born in Durham, NC in 1996. After graduating from high school at Granville Central in Spring 2014, he attended the University of North Carolina at Chapel Hill that fall. During his time there, he later studied abroad at the National University of Singapore and interned at Oak Ridge National Laboratory. Upon graduating in 2018 with a Bachelor of Science in Environmental Science and Mathematics, he returned to Oak Ridge National Laboratory and later joined the CURENT Research Center in Fall 2020 to purse a Master of Science in Electrical Engineering at the University of Tennessee in Knoxville.